Review

Negative Thermal Quenching of Photoluminescence- an Evaluation from Macroscopic Viewpoint

Shirun Yan *

Posted Date: 11 December 2023

doi: 10.20944/preprints202312.0655.v1

Keywords: Reliability assessment; Negative thermal quenching; Consistency of the measurement condition.

Review

Negative Thermal Quenching of Photoluminescence—An Evaluation from Macroscopic Viewpoint

Shirun Yan

Department of Chemistry, Fudan University, Shanghai 200438, China; sryan@fudan.edu.cn

Abstract: Negative thermal quenching (NTQ) denotes that the integral emission spectral intensity of a given phosphor increases continuously with increasing temperature up to a certain elevated temperature. NTQ has been a subject of intensive investigation in recent years and a large number of phosphors were reportedly to have exhibited NTQ. In this paper, a collection of results in the archival literature about NTQ of specific phosphors are discussed from a macroscopic viewpoint in the following three aspects:1) Could NTQ of a given phosphor be reproducible?2) Could the associated data for a given phosphor exhibited NTQ be in line with the law of conservation of energy?3) Could NTQ of a given phosphor be demonstrated in a prototype WLED device? By analyzing typical cases based on common sense, it is hoped to increase the awareness for the issues with the papers reporting NTQ of the specific phosphors based on spectral intensity along with for the importance of keeping stability and consistency of the measurement conditions in temperature-dependent spectral intensity measurement which is a prerequisite for the validity of the measurement results.

Keywords: reliability assessment; negative thermal quenching; consistency of the measurement condition

1. Introduction

Negative thermal quenching (NTQ) of photoluminescence has been a subject of intensive investigation in the past two decades. NTQ refers to that the integral emission spectral intensity (I) of a phosphor gradually increases with the increase of working temperature within a certain temperature range, so that at a very high temperature (e.g. 200 °C), the intensity of the emission spectrum of the phosphor is the same or even higher than at low temperature. In some papers, NTQ was termed as abnormal thermal quenching, zero thermal quenching [1–3], anti-thermal quenching [4], etc. NTQ has been reportedly observed over a wide variety of phosphors, such as those singly-doped with rare earth ion [1–41], transition metal ion [42–57], ns^2 ion (Bi^{3+}) [58–62], doubly-doped and triply-doped with rare earth and transition metal ions [63–72], as well as some undoped metal halide [73,74]. The degree of NTQ, that is, the magnitude of the emission spectral intensity enhancement of the phosphor at high temperatures compared to the value at low temperature, ranged from 0.3% [11] to 34700% [50]. The mechanism proposed for NTQ of specific phosphors were also distinct. Many researchers attributed NTQ to defects in the phosphor which absorb and store the excitation light at low temperature and transfer the energy to the luminescent center at high temperatures [1–40,47]. Some researchers ascribed the NTQ of Mn^{4+}-activated fluoride phosphors to an increase in phonon numbers at high temperatures that makes it possible to gain the parity and spin-forbidden $^2E_g \rightarrow {}^4A_{2g}$ transitions [48–55], while others believed that the details of the phase transition process in $Na_3Sc_2(PO_4)_3:Eu^{2+}$ phosphors caused NTQ [6], etc. Some articles proposed the strategies for designing anti-thermal-quenching phosphors based on the mechanism of NTQ [75,76].

One of the motivations for designing thermal quenching (TQ) resistant phosphors is the application in high-power white light emitting diodes (WLED) and laser-driven lighting, because the temperature of the phosphors during the operation of WLED and laser-driven lighting device is

 doi:10.20944/preprints202312.0655.v1

relatively high. The reports on NTQ of various phosphors seem to imply that fluorescence TQ which is a problem hindering the applications of phosphor in high-temperature circumstances has been solved. It is puzzling and regretful that, to the best of our knowledge, there seems hardly a commercial WLED manufacturer advertising their WLED products that could demonstrate NTQ of phosphors at high current densities yet. At the same time, the validity and reliability of the NTQ mechanisms and experimental results reported in the literature aroused controversy. Hao et al. pointed out that the so-called NTQ of the $Sr_8ZnSc(PO_4)_7:Tb^{3+}$ phosphor caused by energy transfer from defect levels in different depths [37] was not convincing, as the luminescence lifetimes of Tb^{3+} at different temperatures in the article did not support this conclusion [77]. Meanwhile, the temperature dependence of the emission spectra of Tb^{3+} in $Ba_2Y_5B_5O_{17}$ (BYBO) and $Ba_2Lu_5B_5O_{17}$ (BLBO) measured by Hao et al. also showed a similar behavior to $Sr_8ZnSc(PO_4)_7:Tb^{3+}$. Nevertheless, lattice defects due to aliovalent substitutions were not available in BYBO and BLBO [77]. The author of this paper also reviewed and commented on the reports about NTQ for Mn^{4+}-doped fluoride phosphors and Eu^{2+}-doped phosphors. Based on a comprehensive analysis of corresponding experimental data, it was suggested that the mechanisms proposed for NTQ of $Na_3Sc_2(PO_4)_3:Eu^{2+}$ being caused by the phase transformation details [78], of Mn^{4+}-activated fluoride phosphors being due to the increase in phonon numbers at high temperatures [79,80], and of Eu^{2+}-activated phosphors stemming from defect-related energy transfer were unconvincing. It seems difficult for one to attribute the NTQ to an intrinsic property of these phosphors. The NTQ phenomenon observed by the researchers was likely a measurement error caused by the volume change arising from the thermal expansion of the phosphor under investigation during the measurement process [78–81]. The temperature -dependent emission spectral intensity alone seemed not to be a reliable measure for evaluating fluorescence TQ, especially for those phosphors having a larger volume change at elevated temperatures due to thermal expansion or phase transition, since spectral intensity is affected by not only the quantum efficiency (QE) of a phosphor but also some extrinsic factors at elevated temperatures. Only when it is also corroborated by the temperature dependence of the QE and/or lifetime of a given phosphor, or demonstrated in practical applications, could the statement that NTQ of a given phosphor was an intrinsic property of the phosphor hold.

The objective of this paper is to scrutinize typical experimental results in the literature regarding NTQ of specific phosphors from a macroscopic viewpoint in the following three aspects: 1) Could NTQ of a given phosphor be reproducible?2) Could the associated data for a given phosphor exhibited NTQ be in line with the law of conservation of energy?3) Could NTQ of a given phosphor be demonstrated in a prototype WLED device? By analyzing the typical cases based on common sense, it is hoped to arouse reader's reflection and awareness on whether the papers reporting NTQ of the specific phosphors could be trustworthy, and also hoped that the stability and consistency of measurement conditions in the temperature-dependent spectral intensity measurement could attract more attention in order to avoid misleading or hindering truly meaningful researches on anti-TQ phosphors due to plethora of papers in the published literature in which NTQ were achieved based largely on the crude and unreliable temperature-dependent spectral intensity of specific phosphors.

2. Assessment of the selected literature results

2.1. Could NTQ of a given phosphor be well reproducible?

It is generally acknowledged that an essential requirement for experimental results on material properties of scientific significance that deserve discussion is the repeatability. If NTQ is an intrinsic property of a specific phosphor, temperature dependence of the emission intensity of given phosphor measured by different researchers or by the same research group at different times should be reproducible within a reasonable range of uncertainty.

$Na_3Sc_2(PO_4)_3:Eu^{2+}$, a sodium superionic conductor (NASICON)-type phosphor, is one of the most heavily investigated Eu^{2+}-doped phosphors. TQ property of $Na_3Sc_2(PO_4)_3:Eu^{2+}$ was reported by more than five independent research groups during 2016-2022 [1,2,5–8,71]. In particular, the paper authored by Im et al. entitled "A zero- thermal-quenching phosphor" published in "Natural

Preprints (www.preprints.org) | NOT PEER-REVIEWED | Posted: 11 December 2023 doi:10.20944/preprints202312.0655.v1

Materials" in 2017 has been widely cited in the reports on NTQ [2]. Although these authors all claimed that the phase-pure $Na_{3-2x}Sc_2(PO_4)_3$:xEu^{2+} phosphors had a NTQ phenomenon. Nevertheless, both the temperature at which a maximum emission intensity was obtained and magnitude of the maximum emission intensity with respect to the intensity at room temperature, i. e. I_{max}(T), for the $Na_3Sc_2(PO_4)_3$: Eu^{2+} phosphor with the same Eu^{2+} doping concentration reported by different research groups or even by the same research group in different publications were different considerably. Wang et al. reported that, while heating the phosphor from 25 to 250 °C, the emission intensity increased gradually at first and then reached the maximum at 150 °C, upon which the emission intensity started to decrease. The emission intensity of the phosphor with an optimum concentration of Eu^{2+} doping $Na_3Sc_2(PO_4)_3$:0.03Eu^{2+} (NSP:0.03Eu^{2+}) at 150 °C was 110% compared to that at room temperature, as shown in Figure 1a [5]. Im and co-workers reported that the $Na_3Sc_2(PO_4)_3$:0.03Eu^{2+} (NSPO:0.03Eu^{2+}) phosphor showed a ~25% increase in emission intensity in the β-phase (above 65 °C) compared to the RT emission, and reached a maximum at ~164 ºC (β-phase)[2]. Im and co-workers reported recently in another paper that emission intensity of the $Na_3Sc_2(PO_4)_3$:0.03Eu^{2+} increased by about 70% when the temperature was increased from 25 to 150°C, and reached a maximum at about 175 °C, as displayed in Figure 1b [1]. Xian et al. reported that emission intensity of $Na_3Sc_2(PO_4)_3$:0.03Eu^{2+} under 340 nm excitation increased when increasing temperature from 300 up to 425 K. Further increasing temperature led to TQ phenomenon. The emission intensity at 425 K was ~120% compared to the emission intensity at room temperature, as depicted in Figure 1c [8]. Liu et al. reported that integrated luminescence intensity of $Na_3Sc_2(PO_4)_3$: 0.03Eu^{2+} (NSPO:0.03Eu^{2+}) increased by ~30% when the temperature was increased from 30 to 150 °C, as illustrated in Figure 1d [71]. Yan et al. reported that integrated emission intensity of $Na_3Sc_2(PO_4)_3$:0.03Eu^{2+} (NSP: 0.03Eu^{2+}) increased with increasing temperature from 300 up to 425 K, and then decreased when further increasing temperature above 425 K. The emission intensity at 425K was ca. 160% compared with the initial emission intensity at room temperature, as shown in Figure 1e [7].

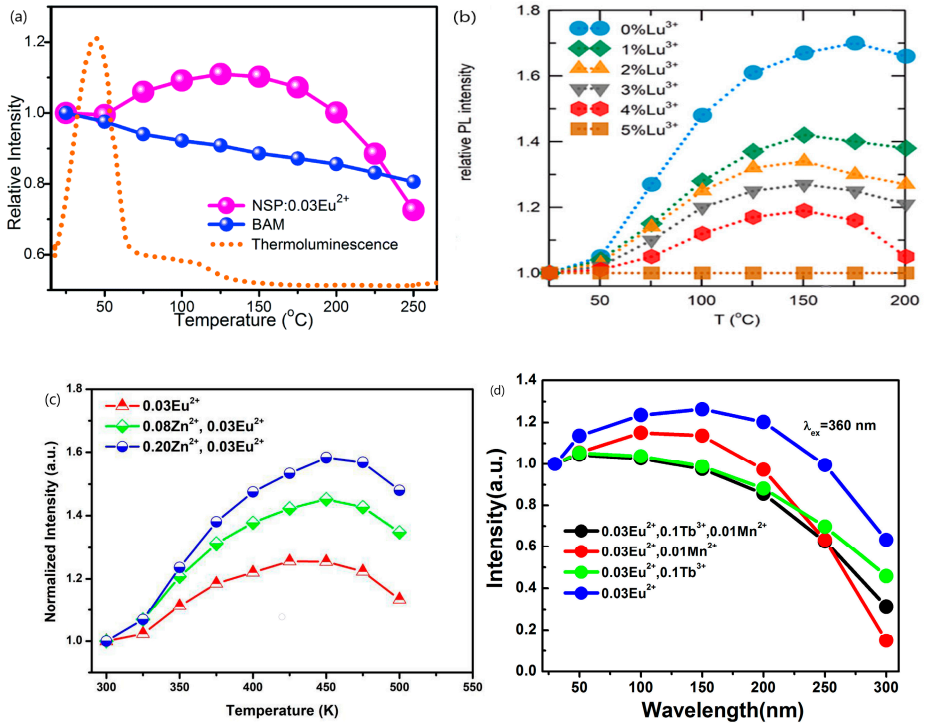

Preprints (www.preprints.org) | NOT PEER-REVIEWED | Posted: 11 December 2023 doi:10.20944/preprints202312.0655.v1

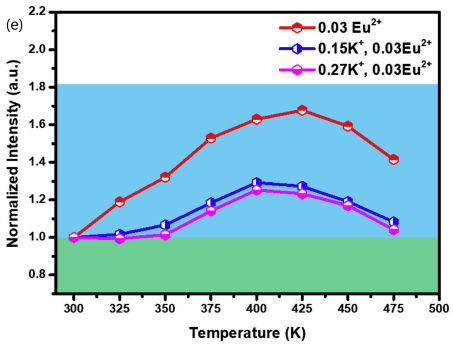

Figure 1. (a) Temperature dependence of the emission intensity of NSP: 0.03Eu^{2+} compared with that of the commercial phosphor BAM. The dotted line represents the thermoluminescence curve of NSP: 0.03Eu^{2+} [5]. (b) Temperature-dependent PL variation of the 450 nm peak of the NSPO:3% Eu^{2+}, yLu^{3+} phosphor as a function of Lu^{3+} concentration [1]. (c) Emission intensity of $Na_3Sc_2(PO_4)_3$: 0.03Eu^{2+}, $Na_3Sc_{1.92}Zn_{0.08}(PO_4)_3$: 0.03$Eu^{2+}$, and $Na_3Sc_{1.80}Zn_{0.20}(PO_4)_3$: 0.03$Eu^{2+}$ from 300 to 500 K, the initial emission intensities at room temperature are normalized to 1 [8]. (d) Temperature-dependence integrated luminescence intensity of NSPO:0.03Eu^{2+} (blue line), NSPO:0.03Eu^{2+}, 0.1Tb^{3+}(green line), NSPO:0.03Eu^{2+}, 0.01Mn^{2+} (red line) and NSPO:0.03Eu^{2+}, 0.1Tb^{3+}, 0.01Mn^{2+} (black line) [71]. (e) Temperature-dependent integrated intensity of NSP: 0.03Eu^{2+}, $K_{0.15}$NSP: 0.03Eu^{2+} and $K_{0.27}$NSP: 0.03Eu^{2+} [7]. Reproduced with permission from the respective references. Copyright 2016 The Royal Society of Chemistry, 2021 American Chemical Society, 2018 The American Ceramic Society and 2019, 2020 Elsevier B.V., respectively.

Mn^{4+}-doped fluorides are a kind of red-emitting phosphors which have been extensively reported to have NTQ [47–56], although many researchers reported normal TQ of Mn^{4+} luminescence [82–88]. Taking the most extensively studied phosphor K_2SiF_6:Mn^{4+} as an example, some researchers reported that the K_2SiF_6:Mn^{4+} showed a normal TQ behavior at high temperatures, analogous to that of most inorganic phosphors [82,86–88]. On the contrary, many researchers reported that the K_2SiF_6:Mn^{4+} phosphor showed an NTQ behavior [47–50,52,53]. However, both the temperature at which a maximum emission intensity observed and the magnitude of the maximum emission intensity with respect to the intensity at room temperature of phase-pure K_2SiF_6:Mn^{4+} phosphor reported by different researchers, or even the same commercial TriGain® K_2SiF_6:Mn^{4+} phosphor measured by the same research group [47,89] were distinct, as illustrated in Figure 2. The author discussed this issue in a previous paper [80].

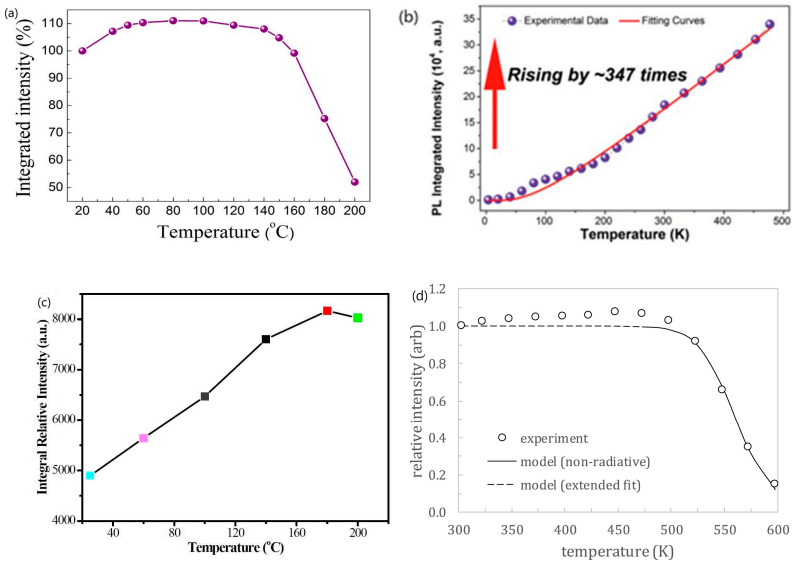

Preprints (www.preprints.org) | NOT PEER-REVIEWED | Posted: 11 December 2023 doi:10.20944/preprints202312.0655.v1

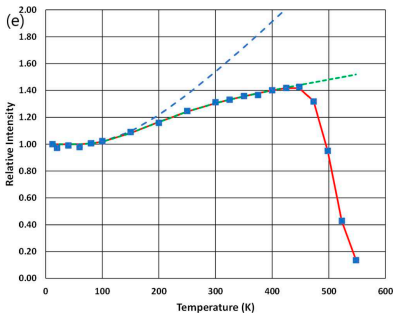

Figure 2. Temperature dependence of emission intensity of $K_2SiF_6:Mn^{4+}$ phosphor reported by different researchers. (a) Ref. [49].(b) Ref.[50].(c) Ref.[52],and of TriGain® commercial phosphor (d) Ref. [89],(e) Ref. [47] (blue squares are experimental intensity).Reproduced with permission from the respective references. Copyright 2016 Elsevier B.V, 2018 American Chemical Society, 2015 The Royal Society of Chemistry, 2018 Elsevier, 2023, The Electrochemical Society,respectively.

Based on the results in Figures 1 and 2, it appears hard for one to draw a conclusion that NTQ phenomenon of either $Na_3Sc_2(PO_4)_3:0.03Eu^{2+}$ or K_2SiF_6: Mn^{4+} phosphor is reproducible within a reasonable range of measurement errors.

2.2. Could the associated data of a specific NTQ phosphor be in line with the law of conservation of energy?

As is well known, phosphors are a kind of frequency (or wavelength) conversion materials. The down-shift phosphors can convert one short wavelength (high frequency) photon to one long wavelength (low frequency) photon. Due to possible non-radiative decay process of the excited state, part of the absorbed energy could be lost in the phosphor as heat. The law of conservation of energy states that when light is absorbed by a phosphor, the energy must go somewhere. Considering that no afterglow luminescence was observed at any temperature in the phosphors reported with NTQ, it means that the light absorption and emission processes do not involve energy storage and a delayed release for these phosphors. Therefore, the sum of the instantaneously emitted energy (E_{Em}) by the phosphor and the energy lost in the phosphor should be equal to the absorbed energy (E_{Abs}) by the phosphor. The energy lost in the phosphor includes the energy lost due to non-radiative decays (E_{NR}) and Stokes shift (E_{SS}). That is, the flow of energy past through a phosphor in a unit time period at any temperature could be expressed by the following equation:

$$E_{Abs}=E_{Em}+E_{NR}+E_{SS} \quad (1)$$

Let's first discuss the left-hand side of energy balance equation (1) for a phosphor. - the absorbed energy by a phosphor (E_{Abs}). Considering that a monochromatic radiation is usually chosen as an excitation light (λ_{exc}) when measuring an emission spectrum, the absorbed energy by the phosphor can be approximated as the product of the energy of single-frequency excitation radiation and the total number of photons absorbed. The number of photons absorbed by the phosphor is proportional to the number of activator centers per unit volume (N) and the transition probability (P_{if}). According to the literature, electric dipole absorption probability of a two-level center in crystal could be expressed as[90]:

$$P_{if}=\frac{\pi}{3n\varepsilon_0 c_0 \hbar^2} I\left|\mu_{if}\right|^2\left(\frac{E_{loc}}{E_0}\right)^2 \delta(\Delta\omega) \quad (2)$$

where $I=\frac{1}{2}nc_0\varepsilon_0E_0^2$ is the intensity of the incident radiation (assuming an incident plane wave), $\hbar$ is the reduced Planck's constant, c_0 is the speed of light in a vacuum, n is the refractive index of the phosphor, and ε_0 is the permittivity in a vacuum, μ_{if} is the matrix element of electric dipole moment, E_{loc} and E_0 are the actual local electric field acting on the valence electrons of the absorbing center due to the electromagnetic incoming wave and the average electric field in the medium, respectively. $\delta(\Delta\omega)$ is the frequency of the incident monochromatic radiation [90]. From Eq. (2) one can hardly expect that the absorption probability increases with increasing temperature.

Preprints (www.preprints.org) | NOT PEER-REVIEWED | Posted: 11 December 2023 doi:10.20944/preprints202312.0655.v1

In fact, the temperature dependence of the absorption intensity of specific phosphors that exhibited NTQ have been investigated by some researchers. Shao et al. investigated temperature-variable diffuse reflection spectra of the K_2SiF_6: Mn^{4+} phosphor in a temperature range from 20 to 80 ºC [49], and found that no obvious changes in absorption rates with increasing the temperature. Im et al. studied the temperature-dependent absorption fraction of $Na_{3-2x}Sc_2(PO_4)_3$: xEu^{2+} (x=0.01, 0.03, 0.07) under 370 nm excitation in the temperature range of 25 – 175ºC with temperature interval of 25 ºC. The results showed that the absorption fraction of the $Na_{3-2x}Sc_2(PO_4)_3$: xEu^{2+} phosphors remained unchanged with rising temperature, suggesting that the enhanced emission intensity does not arise from the increase in absorption fraction [2].

Next, we will discuss the first item on the right-hand side of Eq. (1): the emitted energy by the phosphor (E_{Em}), which is called radiant power measured in joules per second or watt in radiometry. It is easily imagined that the E_{Em} is associated with the emission spectral intensity. Given that in spectral measurement the emission by the phosphor upon excitation is directional-hemispherical while the spectrum recorded by a spectrofluorometer is the radiant power per unit solid angle of a specific direction determined by the geometrical configurations of the spectrofluorometer (radiant intensity), the total radiant power could be obtained by 2π steradian times the radiant intensity [91]. If the emission spectrum is plotted as emitted energy per constant wavelength interval, then

$$E_{Em} = 2\pi \int_{380}^{780} I(\lambda)\, d\lambda \quad (3)$$

where $I(\lambda)$ is the spectral intensity, which is defined as the radiant intensity per unit wavelength interval.

The emitted energy by a phosphor is determined by the number of activator center per unit volume in the excited state(N^*), the probability of radiative transition of the excited electron (P_{fi}), and energy difference between the emitting level of excited and ground states [92,93].

The second term on the right-hand side of Eq. (1), the energy lost in the phosphor due to non-radiative decay (E_{NR}), can be quantified by internal quantum efficiency (IQE), defined as the ratio of the number of emitted quanta to the number of absorbed quanta by the phosphor. The IQE is determined by the probability of radiative and nonradiative decays of the excited center per unit time (i.e., decay rates) and can be expressed as:

$$IQE = \frac{\Gamma_R}{\Gamma_R + \Gamma_{NR}} \quad (4)$$

where Γ_R and Γ_{NR} are the radiative and nonradiative decay rates of the excited center, respectively [48,51]. Eq. (4) indicates that E_{NR} increases when the IQE of a phosphor decreases, and vice versa.

The third term on the right-hand side of Eq. (1), E_{SS}, stems from the interaction between electron in the excited state and the crystal lattice vibrations. Upon excitation from the ground state, the excited electron quickly relaxes into the lowest vibrational level within the excited electronic state, losing some of the initial excitation energy as heat. Subsequently, electron in the lowest vibrational level of the excited state decays to the ground state accompanied with light emission. Vibrational relaxation of the excited electron results in the energy of emitted photons to be less than that of absorbed photons [92–94].

The emission spectral intensity of a phosphor increases with increasing temperature, i.e., NTQ, suggesting that the emitted energy (E_{em}) by the phosphor increases with increasing temperature. If the absorbed energy does not increase, in order to ensure that Eq. (1) holds, the second or/and third terms on the right-hand side of the formula should be decreased in an equal proportion. The third term, Stokes loss, is caused by the interaction between the excited state electron and lattice vibrations. As the temperature increases, lattice vibrations strengthen. It seems difficult for one to expect that the Stokes loss could be decreased with increasing temperature. It has shown that for Eu^{2+} and Ce^{3+}-activated phosphors, the Stokes shift increased with increasing temperature due to an enlarged activator site induced by lattice thermal expansion along with enhanced vibrations at high temperatures [95]. Therefore, it appears that only when the energy lost in the phosphor due to non-radiative decay (E_{NR}) decreases, that is, the IQE increases with increasing temperature, could the above Eq. (1) hold.

To make IQE of a given phosphor increasing with temperature, it requires either the radiative decay rate (Γ_R) increasing with temperature or the non-radiative decay rate (Γ_{NR}) decreasing with

Preprints (www.preprints.org) | NOT PEER-REVIEWED | Posted: 11 December 2023 doi:10.20944/preprints202312.0655.v1

temperature, or concurrent of the two. Nevertheless, for allowed electric dipole transitions, like $4f^{n-1}5d^1 \rightarrow 4f^n5d^0$ transitions of Eu^{2+} and Ce^{3+}-doped phosphors, the radiative decay rate (Γ_R) is constant independent of temperature, it is hard to imagine that radiative decay rate (Γ_R) for these phosphors could increase with increasing temperature. At the same time, the nonradiative decay rate (Γ_{NR}) commonly increases above a critical temperature leading to luminescence TQ. Temperature dependence of nonradiative decay rate can be expressed as [92,93]:

$$\Gamma_{NR}=A \exp(-\Delta E/k_B T) \quad (5)$$

in which A is a constant (units s^{-1}), ΔE is the energy barrier for thermal quenching, k_B is Boltzmann's constant (8.617×10^{-5} $eV.K^{-1}$). Irrespective of the mechanism (or pathway) for non-radiative decay being either multi-phonon emission, crossover of the ground and excited potential curves in the configuration coordinate diagram, or photoionization of 5d electron into the conduction band of the matrix, it is hard to expect that the non-radiative decay rate decreasing with increasing temperature could happen based on Eq. (5).

There were also reports in the literature on the temperature dependence of IQE of some phosphors that showed NTQ in the emission spectral measurements. Zhou et al. reported that the peak intensity and integrated area intensity of $SB_{0.3}PE$ at 150 ºC reached 108% and 124% of the room temperature value, as illustrated in Figure 3a [12]. The IQE of the phosphor at 150 ºC decreased to 85% from the room temperature value 100%, and the absorption of the excitation light within the range of 25-150 ºC was almost constant, as shown in Figure 3b [12]. Figure 3 shows that although the emission spectral intensity increased with increasing temperature, neither the energy absorbed by the phosphor nor the IQE of the phosphor increased with increasing temperature, indicating that a decrease in the energy loss due to non-radiative decay was not observed in this phosphor that exhibited NTQ.

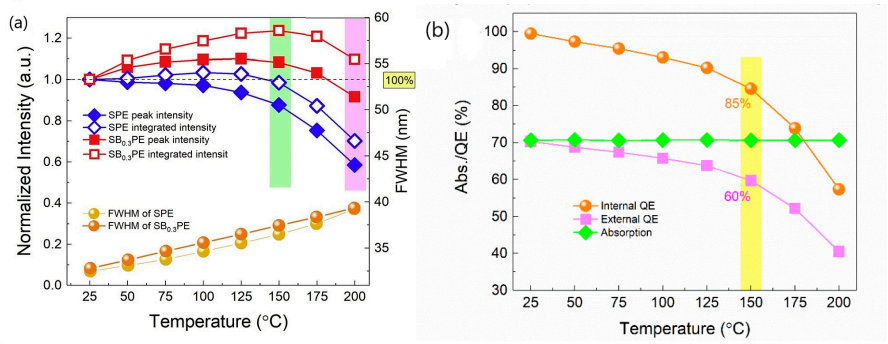

Figure 3. (a) The relationship of peak and integrated intensity, FWHM of SPE, and $SB_{0.3}PE$ versus different temperatures. (b) The variations of IQE, EQE and absorption efficiency of versus temperature from 25 ºC to 200 ºC of $SB_{0.3}PE$ phosphor [12]. Reproduced from Ref. [12].Copyright 2020 The Author(s).

There were also reports in the literature on the temperature dependent QE of $K_2SiF_6:Mn^{4+}$, as illustrated in Figure 4 [82]. It can be seen from Figure 4 that the IQE and EQE of the phosphor maintained almost unchanged with the increase of temperature from room temperature to 150 ºC, indicating that the energy lost in the phosphor due to nonradiative decay did not decrease with the increase of temperature, and the absorption of the excitation light by the phosphor did not increase with the increase of temperature either.

Preprints (www.preprints.org) | NOT PEER-REVIEWED | Posted: 11 December 2023 doi:10.20944/preprints202312.0655.v1

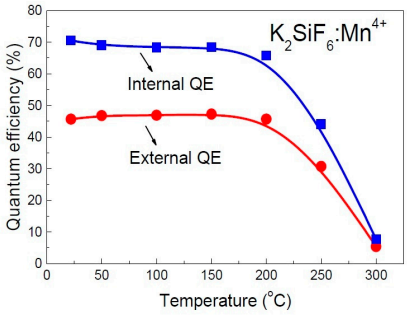

Figure 4. Temperature- dependent IQE and EQE of $K_2SiF_6:Mn^{4+}$ when excited at 450 nm [82]. Reproduced from Ref.[82] with permission, Copyright 2015 Optical Society of America.

The results in Figures 3 and 4 reveal that the variation of IQE with temperature showed a different trend from that of the emission spectral intensity, suggesting that these data could hardly be in line with Eq. (1).

2.3. Could NTQ of a given phosphor be demonstrated in prototype WLED device?

The aim of phosphor researches lies not only in exploring the theoretical issues underlying, but also in finding practical applications for specific phosphors. If a phosphor possesses a peculiar attribute, in addition to be proven by characterizations, it should also be demonstrated in practical applications. One of the motivations for designing TQ resistant phosphors is the application in high-power WLED and/or laser-driven lighting, because the temperature of the phosphors during the operation of WLED or laser-driven lighting is relatively high [94]. If the QE of the phosphors decreases at working temperature, the efficiency and color of the device will change. Generally, four metrics – luminous efficacy, the color-rendering index (CRI), correlated color temperature (CCT), lifetime, are used to describe the performance of a WLED device [94]. The luminous efficacy expressed in lumens per watt, is a parameter describing how bright the radiation is perceived by the average human eye. It scales with the eye sensitivity curve $V(\lambda)$ and can be calculated from the emission spectrum $I(\lambda)$. As the eye sensitivity peaks at 555 nm, the fraction of green-yellow light, along with its wavelength and IQE have the greatest impact on luminous efficacy of WLED. The CRI quantifies the color-rendering ability or color reproducibility of a white light source scored on a scale from 0 (no color reproducibility) to 100 (perfect reproducibility, achieved by black body radiators). The CCT describes the hue of the white light. The lower CCT value represents the warmer light (being yellower) while the higher CCT value denotes the cooler light (being bluer). Generally, the CCT of a WLED device is largely determined by the fractions of red and blue light in the white spectrum. An increase in CCT means that the either fraction of the blue light in the white spectrum increases, or the fraction of the red light decreases. On the contrary, a decrease in CCT means that the fraction of the red light in the white spectrum increases, or the fraction of the blue light decreases. [94,96]. Given that the main concern of this paper is whether the phosphor that exhibited NTQ in temperature-dependent spectral measurement could demonstrate a similar performance in a prototype WLED device along with that the emitting colors of the phosphors discussed in this paper which reportedly exhibited NTQ are dominantly blue and red, we focus our discussion on the variation of CCT of the prototype WLED device at different driven currents.

Table 1 compiles the results reported in the literature about chromaticity coordinate and CCT of four prototype WLED devices fabricated by coating an InGaN blue chip or an UV chip using the phosphor blend containing specific phosphors which showed NTQ in the spectral measurement under different drive currents. No.1 and No.2 devices are composed of a blue chip and the phosphor blend in which the red-emitting phosphor $K_2TiF_6:Mn^{4+}$ [48,51–53] and $K_3AlF_6:Mn^{4+}$ [97–99] have been reported by multiple independent research groups to exhibit NTQ in the spectral measurements. No.3 and No. 4 devices are composed of an UV chip and the phosphor blend in which the blue-emitting phosphor $Na_3Sc_2(PO_4)_3:0.03Eu^{2+}$ (NSPO:Eu^{2+}) and $Sr_{1.38}Ba_{0.6}P_2O_7:0.02Eu^{2+}$ ($SB_{0.3}PE$) have been

Preprints (www.preprints.org) | NOT PEER-REVIEWED | Posted: 11 December 2023 doi:10.20944/preprints202312.0655.v1

reported by multiple independent research groups to exhibit NTQ in spectral measurements [1,2,5–8,12]. Could the red-emitting phosphors or blue emitting phosphors exhibit NTQ in the respective WLED device?

As has been discussed earlier, if emission intensity of the red-emitting phosphor increases with temperature while the emission intensity of the blue-emitting phosphor decreases with increasing temperature (normal TQ), the CCT of the WLED is expected to decrease at elevated temperatures. If emission intensity of the blue-emitting phosphor increases with temperature while emission intensity of the red-emitting phosphor decreases with temperature, the CCT of the WLED is expected to increase at high temperatures. If the quenching rate with temperature of the blue-emitting and red-emitting phosphors is the same, the CCT of the WLED changes little with temperature.

Table 1. Chromaticity coordinate and CCT of the WLEDs device fabricated using specific phosphors which showed ATQ in spectral measurement under different drive currents. [a]

No	Composition of WLED	Drive current/mA	Chromaticity coordinate		CCT/K	Ref.
			x	y		
1	Blue chip (λ=455nm) + YAG 04 + **$K_2TiF_6:Mn^{4+}$**	20	0.4575	0.4124	2748	51
		40	0.4588	0.4160	2757	
		60	0.4569	0.4158	2783	
		80	0.4539	0.4152	2821	
		100	0.4550	0.4172	2820	
		120	0.4534	0.4158	2833	
2	Blue chip + YAG:Ce^{3+} (0.1g) + **$K_3AlF_6:Mn^{4+}$** (0.4g)	40	0.4208	0.4014	3270	98
		120	0.4178	0.3951	3275	
		240	0.4142	0.3874	3284	
		300	0.4127	0.3832	3278	
3	UV chip (λ=365 nm) + **$Na_3Sc_2(PO_4)_3:0.03Eu^{2+}$** + $La_3Si_6N_{11}:Ce^{3+}$ + $(Sr,Ca)AlSiN_3:Eu^{2+}$	100	0.2989	0.3502	7041[b]	2
		200	0.2968	0.3531	7116	
		300	0.2958	0.3574	7121	
		400	0.2952	0.3602	7121	
		500	0.2953	0.3617	7101	
		600	0.2957	0.3625	7075	
		700	0.2963	0.3632	7040	
		800	0.2970	0.3633	7006	
		900	0.2975	0.3639	6978	
		1000	0.2982	0.3639	6945	
4	UV chip (λ=365 nm) + **$Sr_{1.38}Ba_{0.6}P_2O_7:0.02Eu^{2+}$** + $(SrBa)_2SiO_4:Eu^{2+}$ + $(Sr,Ca)AlSiN_3:Eu^{2+}$	25	0.3958	0.4065	3831	12
		50	0.3957	0.4050	3823	
		75	0.3957	0.4036	3814	
		100	0.3956	0.4028	3811	
		125	0.3955	0.4019	3807	
		150	0.3955	0.4008	3799	
		175	0.3956	0.3997	3789	
		200	0.3958	0.3984	3775	

[a]: The formula of the phosphor which showed NTQ in spectral measurement was highlighted in bold. [b]:CCT values are calculated from the chromaticity coordinates x and y given in Supplementary Table S5 of Ref. [2] according to McCamy's formula [100]: $T\ (K) = -449n^3 + 3525n^2 - 6823.3\ n + 5520.33$. where n= (x-0.3320)/(y-0.1858).

Table 1 shows that the CCT of No.1 WLED increased gradually when the drive current increased from 20 to 120 mA, while the CCT of No.2 WLED increased steadily with increasing drive current from 40 to 240 mA. With further increasing drive current from 240 to 300 mA, the CCT of No. 2 WLED decreased. The variation of CCT with drive current of these two WLED devices indicates that the fraction of the red light in the spectrum of these two WLED decreased with increasing drive current below 240 mA, implying that NTQ of the respective red-emitting phosphor, i.e., the emission

Preprints (www.preprints.org) | NOT PEER-REVIEWED | Posted: 11 December 2023 doi:10.20944/preprints202312.0655.v1

intensity increasing with temperature could hardly be substantiated by its performance in these two WLED devices.

It is worth mentioning that, in addition to TQ, excitation saturation may also result in a decrease in luminescence efficiency (droop) of the specific phosphor at high drive current of WLED. The excitation saturation refers to that the luminescence intensity of a phosphor does not linearly increase with the increase of excitation power. The excitation saturation is generally caused by ground-state depletion and associated with luminescence lifetime of the phosphor [94,101,102]. The luminescence lifetime of Mn^{4+} -activated phosphors (ms at room temperature) is longer than that of Ce^{3+}-activated phosphors (ns) and Eu^{2+}-activated phosphor (μs) [48,81,103]. Experimental results showed that Mn^{4+}-activated fluorides had considerably lower threshold for excitation saturation than that of Eu^{2+} and Ce^{3+} -activated phosphors in WLED [88,104,105]. It is not clear which drive current is the onset of excitation saturation for these two red-emitting phosphors in No.1 and No.2 WLED devices and to what extent the excitation saturation also contributed the increase in the CCT of No.1 and No.2 WLED devices at high drive current given that the blue light in these two WLEDs was provided by a InGaN chip which also suffers from the external quantum efficiency drop when increasing drive current above a critical value [106].

The data in Table 1 show that the CCT of No. 3 WLED gradually increased from 7041 K to the maximum 7121 K when the drive current increased from 100 mA to 300 mA. The CCT monotonically decreased with further increasing the drive current above from 400 mA, indicating that the fraction of the blue light in the WLED spectrum decreased with increasing drive current above 400 mA, that is NTQ of the blue emitting phosphor $Na_3Sc_2(PO_4)_3$:0.03Eu^{2+} could hardly be substantiated by its performance in WLED device above 400 mA. If the blue-emitting phosphor had NTQ, i.e., emission intensity increasing with increasing temperature, the CCT of the WLED should increase as well [94]. Given that the blue-emitting phosphor $Na_3Sc_2(PO_4)_3$:0.03Eu^{2+} and red-emitting phosphor (SrCa)$AlSiN_3$:Eu^{2+} in No. 3 WLED contain the same activator (Eu^{2+}) with similar luminescence lifetime, excitation saturation could not be the issue resulting in decrease in CCT with increasing drive current of No. 3 WLED.

In addition to luminescence TQ and excitation saturation, another possible reason that could cause decrease in the fraction of the blue light under high drive current is an increased reabsorption process of the other additive phosphor components. In the supplementary information, Im et al. mentioned that the excitation spectrum of the yellow-emitting $La_3Si_6N_{11}$:Ce^{3+} and red-emitting (SrCa) $AlSiN_3$: Eu^{2+} overlapped with the emission spectrum of $Na_3Sc_2(PO_4)_3$:0.03Eu^{2+} phosphor, and there was a significant absorption of the blue component of $Na_3Sc_2(PO_4)_3$:0.03Eu^{2+} phosphor by the yellow-emitting $La_3Si_6N_{11}$:Ce^{3+} phosphor and red-emitting (SrCa)$AlSiN_3$:Eu^{2+} phosphor, resulted in the decrease of blue component during WLED fabrication [2]. If the absorption of blue light by the red-emitting or/and yellow-emitting phosphor enhances at high temperatures, even if the blue-emitting phosphor $Na_3Sc_2(PO_4)_3$:0.03Eu^{2+} had no TQ at high drive current, an enhanced reabsorption by the red and/or yellow-emitting phosphor could also result in a decrease in the fraction of the blue light in WLED device. Then, could the decrease in CCT of No.3 WLED device under high operating current be caused by the enhanced reabsorption of the red or/and yellow-emitting phosphor?

There were no reports in the literature on the temperature-dependent excitation spectra of (SrCa) $AlSiN_3$:Eu^{2+} and $La_3Si_6N_{11}$:Ce^{3+} phosphors. As mentioned earlier, the absorption intensity of Eu^{2+} and Ce^{3+}-doped phosphors is determined by the number of activator centers per unit volume and the transition probability from the ground state to the excited state. On the one hand, multiple independent researchers confirmed that both the yellow-emitting phosphor $La_3Si_6N_{11}$:Ce^{3+}[107,108] and the red emitting phosphors $CaAlSiN_3$:Eu^{2+} and (SrCa)$AlSiN_3$:Eu^{2+} [109,110] exhibited TQ, and the mechanism of TQ was generally believed to be thermally-assisted photoionization of 5d electrons of the activator ion (Ce^{3+}, Eu^{2+}), suggesting that the number of the activator centers per unit volume could hardly increase with increasing temperature. On the other hand, the light absorption of (SrCa) $AlSiN_3$: Eu^{2+} and $La_3Si_6N_{11}$:Ce^{3+} phosphors originates from the parity-allowed $4f^n5d^0 \rightarrow 4f^{n-1}5d^1$ electric dipole transition of respective Eu^{2+} and Ce^{3+} ions, whose transition probability could be expressed by Eq. (2) and independent of temperature. In terms of either the number of activator center in unit

Preprints (www.preprints.org) | NOT PEER-REVIEWED | Posted: 11 December 2023 doi:10.20944/preprints202312.0655.v1

volume or transition probability, it seems difficult to predict theoretically that the absorption of the blue light by the yellow-emitting and/or red-emitting phosphors will increase with increasing temperature.

Multiple independent research groups reported on the absorption spectra of $Y_3Al_5O_{12}$: Ce^{3+}(YAG: Ce^{3+}) [111,112] and $Y_3Ga_5O_{12}$: Ce^{3+} (YGG: Ce^{3+}) [113] phosphors at different temperatures, as shown in Figure 5a,b. YAG:Ce^{3+} and YGG:Ce^{3+} showed two intense bands within the measured range of the absorption spectra, which can be attributed to the transition from the ground state ($4f^1$) to the two lowest-lying $5d^1$ states of the Ce^{3+} ion. As the temperature increased, the intensity of absorption band in the blue region corresponding to the transition from the $4f^1$ to the lowest-lying $5d^1$ state of the Ce^{3+} ion decreased gradually, suggesting unambiguously that absorption of blue light decreased with increasing temperature in the temperature range investigated [111–113]. The excitation spectrum of $La_3Si_6N_{11}$:Ce^{3+} shown in Figure 5c [114] resembles the excitation spectra of YAG: Ce^{3+} and YGG: Ce^{3+}. There were also two absorption bands in the blue and nUV regions corresponding to the transition from the ground state of the Ce^{3+} ion ($4f^1$) to the two lowest-lying $5d^1$ states. It seems reasonable to infer that temperature-dependence of the excitation (absorption) spectrum of the $La_3Si_6N_{11}$:Ce^{3+} phosphor should be similar to that of YAG:Ce^{3+} and YGG:Ce^{3+}, that is, the absorption intensity of the blue light should not increase with increasing temperature.

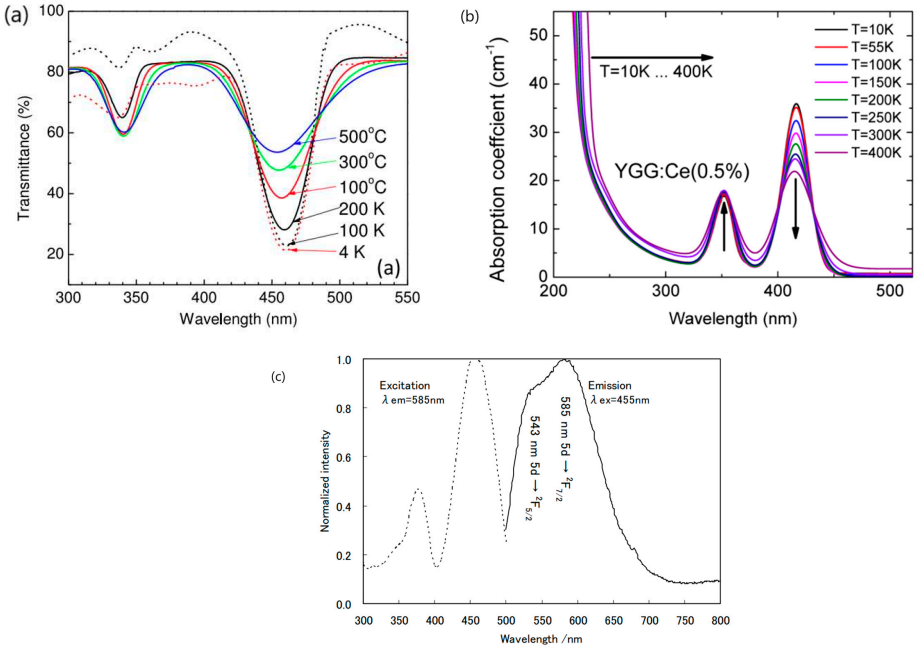

Figure 5. (a) Transmittance spectra of Ce:YAG from low to high temperature [111]. (b) Temperature dependence of the UV and VIS absorption spectra of the YGG:Ce (0.5%) crystal [113].(c) Excitation and emission spectra of $La_{2.94}Ce_{0.06}Si_6N_{11}$ synthesized at 1950℃ for 2 h under nitrogen atmosphere of 0.92 MPa [114].Reproduced with permission from respective references, Copyright 2015 IOP Publishing Ltd ,2015 Optical Society of America,2009 ECS - The Electrochemical Society,respectively.

The temperature-dependent excitation spectra of red-emitting phosphor $CaAlSiN_3$:Eu^{2+} were reported by Chen et al., as shown in Figure 6 [115]. It is evident that the excitation intensity of $CaAlSiN_3$:Eu^{2+} phosphor by the blue light did not increase with increasing temperature from 20 to 300 K. It seems reasonable to suggest that the variation of the excitation spectrum of (SrCa)$AlSiN_3$: Eu^{2+} phosphor with temperature should have a similar to trend to that of $CaAlSiN_3$:Eu^{2+}. The results in Figures 5 and 6 indicate that the decrease in CCT of No.3 WLED device at high drive current seems unlikely to be caused by an increased absorption of the blue light by the yellow-emitting phosphor $La_3Si_6N_{11}$:Ce^{3+} or/and red-emitting phosphor (SrCa) $AlSiN_3$: Eu^{2+} at high temperatures.

Preprints (www.preprints.org) | NOT PEER-REVIEWED | Posted: 11 December 2023 doi:10.20944/preprints202312.0655.v1

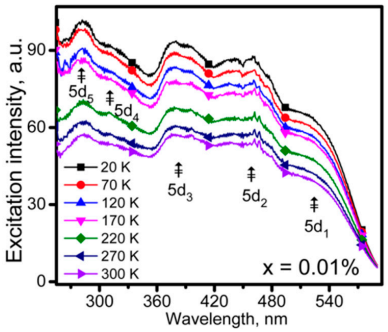

Figure 6. Excitation spectra of $Ca_{0.99}Eu_{0.01}AlSiN_3$ measured at various low temperatures [115].

Reproduced with permission from Ref. [115], Copyright 2016 American Chemical Society.

Given the above discussion, it appears that attributing the decrease in CCT with increasing drive current for No.3 WLED device in Table 1 to either excitation saturation or increased reabsorption process of the other additive phosphor components is unconvincing. The reason for the decrease in CCT of the WLED device at high drive current should be that the blue-emitting phosphor $Na_3Sc_2(PO_4)_3$:0.03Eu^{2+} suffered from severer fluorescence TQ than that of the red-emitting phosphor. This indicates that NTQ of the blue-emitting phosphor $Na_3Sc_2(PO_4)_3$:0.03Eu^{2+} could not be proven by its performance in the prototype WLED device under high drive current.

$Sr_{1.38}Ba_{0.6}P_2O_7$:0.02Eu^{2+} (abbreviated as $SB_{0.3}PE$) was also a blue-emitting phosphor with emission maximum at wavelength 420 nm under nUV excitation which reportedly exhibited NTQ. The temperature- dependent emission spectral measurement showed that the peak intensity and integrated area intensity at 150 ºC reached 108% and 124% of the room temperature values, respectively, as shown in Figure 3a [12]. Could NTQ of $Sr_{1.38}Ba_{0.6}P_2O_7$:0.02Eu^{2+} be demonstrated in the prototype WLED device?

No. 4 WLED device listed in Table 1 was fabricated by coating a 365 nm nUV chip with the phosphor blend containing the blue-emitting ($Sr_{1.38}Ba_{0.6}P_2O_7$:0.02Eu^{2+}) ($SB_{0.3}PE$), yellow-emitting $(SrBa)_2SiO_4$:Eu^{2+} and red-emitting (SrCa) $AlSiN_3$:Eu^{2+}. The drive current dependent CCT of WLED showed the CCT of No.4 WLED monotonically decreased from 3831 K to 3775 K when the drive current increased from 25 mA to 200 mA, suggesting that the fraction of the blue light component in the white spectrum gradually decreased with the increase of the drive current. The decrease in the fraction of the blue light component in the white spectrum could also be seen from the variation of intensity with drive current for the three phosphors in the blend shown in Figure 7. Based on an analogous reasoning to that in No. 3 WLED of Table 1, it seems reasonable to deduce that the decrease in the blue light fraction in No.4 WLED as the drive current increased could hardly be ascribed to either the excitation saturation or absorption by the yellow-emitting phosphor $(SrBa)_2SiO_4$:Eu^{2+} and/or red-emitting phosphor (SrCa) $AlSiN_3$:Eu^{2+}. The most likely reason for the decrease in the fraction of the blue light component in the white spectrum is that the blue emitting phosphor $Sr_{1.38}Ba_{0.6}P_2O_7$:0.02Eu^{2+} suffered from severer TQ than that of the red-emitting phosphor (SrCa)$AlSiN_3$:Eu^{2+}. The fact that the blue emitting phosphor $Sr_{1.38}Ba_{0.6}P_2O_7$:0.02Eu^{2+} suffered from severer TQ than that of the red-emitting phosphor (SrCa)$AlSiN_3$:Eu^{2+} suggest that NTQ of the blue-emitting phosphor $Sr_{1.38}Ba_{0.6}P_2O_7$:0.02Eu^{2+}($SB_{0.3}PE$) could not be demonstrated in high-power WLED device.

Preprints (www.preprints.org) | NOT PEER-REVIEWED | Posted: 11 December 2023 doi:10.20944/preprints202312.0655.v1

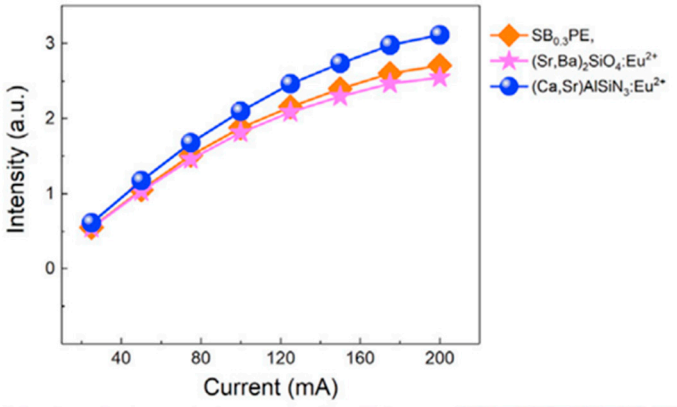

Figure 7. The emission intensities of $SB_{0.3}PE$ blue, $(SrBa)_2SiO_4:Eu^{2+}$, and (SrCa) $AlSiN_3:Eu^{2+}$ phosphors as a function of driving current [12]. Reproduced from Ref. [12]. Copyright 2020 The Author(s).

3. Discussion

Based on the above discussion, it appears reasonable to note that in terms of either the reproducibility of the experimental results, associated data being able to comply with the energy conservation, demonstrability in practical applications of prototype WLED device, the NTQ of these phosphors, despite having been extensively reported by numerous researchers and heavily cited in the literature, could hardly be substantiated. The key reason for this situation, in my opinion, is that the NTQ reported in the literature was based largely on the temperature-dependent emission spectral intensity of the specific phosphor. However, the temperature-dependent emission spectral intensity is not a reliable measure for evaluating luminescence TQ [81]. The contribution of the change in geometrical configuration to the emission spectral intensity at elevated temperatures has been ignored or underestimated.

It is generally acknowledged that QE is a critical parameter for evaluating the performance of phosphor materials, as it indicates their ability to absorb and convert photons to longer wavelengths. IQE and EQE are two commonly used metrics. To evaluate the quality of a given phosphor at room temperature, one should measure the IQE rather than absolute emission spectral intensity of the phosphor. Because a conventional spectrofluorometer can detect only a certain fraction of the emitted light. The size of this fraction depends on many different factors, including the numerical apertures for excitation and the solid angle for detection, the emission wavelength, the emission anisotropy, the scattering of the sample and the sample geometry, and sensitivity and linearity of the detector etc., it is thus impossible to quantify. A recent work by Song et al. demonstrated that even using a commercial spectrofluorometer under the same conditions (slit width, dwell time, scan range, and sample position) operated by the same experimenter, the different quartz lids pairs of the sample chamber resulted in an integrated emission spectral intensity variance of more than 10% for the yellow- and red-emitting phosphors recorded by a PMT (Photomultiplier tube) of the spectrofluorometer [116]. Therefore, investigation of QE of a phosphor by comparison of integral emission spectra (intensity) of the sample and the reference measured using a spectrofluorometer has scientific significance only when the emission spectra were obtained under rigorously identical measurement conditions for the samples of known absorption factors at the excitation wavelength [117]. Keeping consistency and stability of the measurement conditions is crucial to the accuracy and reliability of the emission spectral intensity.

However, it is a great challenge to maintain consistency and stability of the measurement conditions especially surface morphology of the sample and geometrical configuration of the spectrofluorometer at different temperatures when measuring the temperature-dependent emission

 doi:10.20944/preprints202312.0655.v1

spectral intensity using a conventional spectrofluorometer equipped with a temperature control accessory. The main reasons are as follows [80,81]:

1) The measurement of temperature-variable emission spectra from room temperature to specific higher temperature (e.g. 200 ºC) involves multiple sample temperature-rising and temperature-holding steps, and hence is a time consuming process. Maintaining the stability of the excitation source power, detector sensitivity, and other measurement conditions without any fluctuation throughout the whole process is a challenge.

2) In the majority of cases, phosphor expands with increasing temperature, since an increase in energy results in an increase in equilibrium spacing of the atomic bonds. The optical quartz lid of the sample holder (or sample chamber) for masking phosphor samples is an elastic material that could hardly prohibit the phosphor sample from expanding upon heating at ambient pressure. Given that the chemical composition homogeneity and/or particle size uniformity of phosphor samples prepare by laboratory-scale solid state reaction could hardly be always ensured along with that the phosphor powders are randomly packed in the sample holder, thermal expansion (volume change) of the phosphor undoubtedly leads to changes in the state of the sample in directions parallel to and perpendicular to the sample surface. On the one hand, the volume change of the sample in the direction parallel to the surface will cause the state of the sample (packing density and flatness) within cross-sectional area of the incident beam being different from that at low temperature, leading to a change in the reflection/absorption ratio of the phosphor sample and consequently a change in the emission spectral intensity. On the other hand, the volume change in the direction perpendicular to the sample surface will affect the distance from the excitation source to the sample surface and from the sample surface to the detector even though the excitation source, sample holder of the spectrofluorometer could maintain static at fixed positions at elevated temperatures. Consequently, the incident excitation intensity on the phosphor and the emission intensity received by the detector will be biased due to the inverse square law. The magnitude of these changes is associated with the thermal expansion coefficient (lattice rigidity) of the given phosphor, the volume of the sample chamber, the particle size and packing density of the phosphor sample and could hardly be quantified [80]. Either a change in the sample state and surface flatness within the cross-sectional aera of the incident excitation light or a change in geometric configuration of the spectrofluorometer means that the measuring conditions at elevated temperatures have been changed considerably from that at low temperature and hence the emission spectral intensity obtained is unable to accurately characterize the performance of the phosphor any more. Regardless of the volume change of the phosphor was caused by thermal expansion, negative thermal expansion or phase transformation [1,2,6], the change in crystal cell volume of the phosphor at elevated temperatures makes it difficult to maintain the consistency and stability of the measuring conditions in temperature-variable emission spectral measurement.

3) Given that chemical composition homogeneity and/or particle size uniformity of phosphor samples prepare by laboratory-scale solid state reaction could hardly be always ensured [118], the surface of phosphor sample is not an ideal Lambertian surface. The change in the surface state originating from volume change due to thermal expansion or negative thermal expansion may results in a change in the distribution of the emission in different direction, resulting in a change in the intensity received by the detector in the specified direction of the spectrofluorometer irrespective of whether or not the emitted intensity changes with temperature.

4) Due to the thermal expansion or negative thermal expansion of the phosphor sample, the length of the atomic bonds between the activator ion and the ligands will change. For some phosphors, the energetic position of the transitions from the ground state to the excited states is extremely sensitive to the coordination field of the activator ion (such as $4f^n5d^0 \rightarrow 4f^{n-1}5d^1$ transition of Ce^{3+} and Eu^{2+} ions, $^4A_2 \rightarrow {}^4T_2$ transition of Mn^{4+}, and charge transfer from the ligand to Eu^{3+} etc.). The change in the length of the atomic bonds between the activator ion and the ligands may lead to a shift in the excitation band at high temperature from that at low temperature, resulting in change in the absorption of monochromatic excitation light [80,81].

 doi:10.20944/preprints202312.0655.v1

As has been discussed earlier, the key reason for emission spectral intensity at room temperature unable to be an international interlaboratory comparable quantity is that the emission spectral intensity measured is only a certain fraction of the emitted light, and the size of this fraction depends on many different factors. It is impossible to maintain these factors and measuring conditions quantitively identical and consistency universally. The above discussion suggests that during the measurement of variable temperature emission spectra of phosphors using a commercial spectrofluorometer by an experimenter, the consistency and stability of measuring conditions especially the surface state (density and flatness) within the cross-sectional aera of the incident beam and measuring geometry (source-sample distance, sample-detector distance, and angular distribution of emission) could hardly be ensured, especially for those phosphors which have considerable volume changes due to either thermal expansion, negative thermal expansion or phase transformation process. In this case, the measurement errors originating from the volume change make the emission spectral intensity measured at elevated temperatures biased considerably from the emitted intensity by the phosphor. Hence, comparison of emission spectral intensity at higher temperature with respect to the value at low temperature could not truly characterize the change in light conversion efficiency of the given phosphor.

Multiple independent research groups investigated the variation of the emission intensity of the phosphor sample with temperature during heating and cooling processes, and the results are exemplified in Figure 8 [12,18,119]. It can be seen in Figure 8 that the emission intensity of a given phosphor at room temperature increased considerably after the heating- cooling cycles compared to the initial value of the pristine sample. The enhancement of emission spectral intensity at room temperature after heating-cooling cycle in my opinion likely stemmed from the change in the surface state of the sample along with in the geometric configuration of the spectrofluorometer arising from the irreversible change of the sample volume during heating and cooling cycles due to irregular packing. Because these Eu^{2+}-activated phosphors were prepared by solid-state reactions at a temperature above 1200 ºC in reducing atmosphere, the possibility of improving the QE of these phosphors after undergoing heating and cooling cycles in ambient atmosphere in the spectral measurements is extremely low. This also suggests that the intensity enhancement of these phosphors at elevated temperatures likely arose from the same reasons, that is, NTQ, an increase in emission spectral intensity at high temperatures could also originate from the change in packing density and surface state of the sample or in geometrical configuration of the spectrofluorometer not necessarily from an enhanced conversion efficiency of the phosphor. Therefore, temperature-dependent emission spectral intensity could not be a reliable measure for evaluating fluorescence TQ.

Preprints (www.preprints.org) | NOT PEER-REVIEWED | Posted: 11 December 2023 doi:10.20944/preprints202312.0655.v1

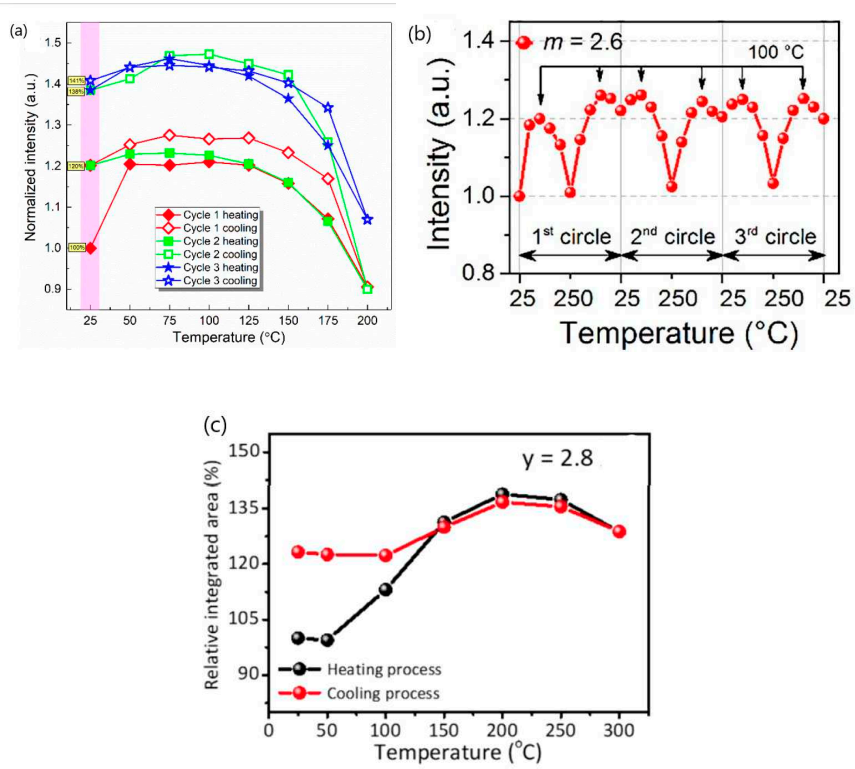

Figure 8. (a) Thermal degradation tests of SB$_{0.3}$PE ((Sr$_{0.69}$Ba$_{0.3}$)$_2$P$_2$O$_7$:0.02Eu^{2+}) phosphor by heating and cooling phosphor for 3 times [12]. (b) Normalized integrated PL intensity versus temperature with 3 heating–cooling circles of K$_{2.2}$Al$_{11}$O$_{17+\delta}$:0.2Eu^{2+} (m = 2.6) [18]. (c)The correlation between the heating and cooling process of the Na$_{2.87}$Sc$_2$(PO$_4$)$_{2.8}$:0.13Eu^{2+} phosphor by the relative-integrated area series [119]. Reproduced with permission from respective references. Copyright 2020 The Author(s), 2021 Elsevier B.V., and 2022 The Royal Society of Chemistry, respectively.

IQE that presents a direct measure for the efficiency of the conversion of absorbed photons into emitted photons is one of the spectroscopic key parameters of phosphors. IQE of a phosphor is customarily measured by an integrating sphere setup by either a "two measurement" or a "three measurement" approach [120,121]. In the two measurement approach, both an empty sphere measurement and a measurement with the sample in the sphere with the excitation beam incident on the sample are performed. In the three measurement approach, an additional measurement with the sample in the sphere, but out of the excitation beam, is performed [121]. Unlike a spectrofluorometer which only detects a certain fraction of the emitted light, an integrating sphere setup captures the total amount of light emitted from the excited sample or scattered by the sample and hence allows for the absolute measurement of the number of emitted photons and the number of absorbed photons. The number of absorbed photons follows from the decrease in the incident excitation light intensity (measured with a blank at the sample position) caused by the absorbing sample in the integrating sphere setup. The integrating sphere setup is insensitive to the alignment of a beam and optical components and hence measurement results are highly repeatable.

IQE can also be determined by measuring the lifetime (τ) being the reciprocal of the sum of the rates of radiative decay (Γ_R) and nonradiative (Γ_{NR}) of the excited center if the lifetime without nonradiative decay (τ_0) is known. Based on the definition of lifetime, Eq. (4) could be modified as:

$$IQE = \frac{\tau}{\tau_0} \quad (6)$$

The IQE of the phosphor could also be determined by relative method, i.e., comparison of integral emission spectra of the sample and the standard under identical measurement conditions for samples of known absorption factors at the excitation wavelength. This requires not only a standard with known QE and with optical properties closely matching those of the investigated sample

 doi:10.20944/preprints202312.0655.v1

properties, but also the measurement of the sample and standard being under identical conditions [117]. If the measuring conditions have changed, validity and accuracy of the relative QE could not be ensured [122].

Spectrofluorimetry is an important tool for phosphor research. Emission spectra can provide important information about the nature and energy of the emitting excited state. The shape of the spectra (narrow line or broad band) indicates the emission either originating from an allowed or a forbidden transition, while the centroid wavelength of the emission represents the energy difference between the ground and excited levels of the emitting center. The full width at half maximum (FWHM) of the emission carries information regarding the uniformity of the surrounding environment of the emitting center, and so on. However, emission spectral intensity gives little information about the conversion efficiency of the phosphor. If one hopes to study the conversion efficiency by comparing the relative emission spectral intensity of the sample with that of the reference standard, not only the measurement of the sample and standard should be performed under identical conditions, but also optical properties of the standard should closely match those of the investigated sample.

Luminescence TQ refers to the drop of conversion efficiency of the given phosphor due to the onset and enhancement of non-radiative decay at elevated temperatures. Investigating into the TQ property of phosphors by measuring the temperature-dependent emission spectral intensity is based on the assumption that variation of integral emission spectra with temperature could represent the variation of IQE with temperature of the phosphor investigated. Unfortunately, the variation of the surface state and geometrical configuration associated with the volume change of the sample at high temperatures invalidates this assumption.

Quantitative luminescence measurements at varying temperatures are often not as easy as they could seem at a first glance, since the electric signal produced by a spectrofluorometer is related to the total luminescence intensity through a number of instrumental factors and, in addition, can often hide artifacts. Many method-inherent problems were often neglected, resulting in measurements that are unreliable and of poor quality.

It is worth noting that the validity of experimental results derived from the temperature-dependent emission spectra depends on the information of interest. If the information of interest is the variation with temperature of the energy position of the emission, FWHM, or relative intensities of multiple peaks in a spectrum, uncertainty caused by changes in surface state of the sample or geometrical configuration of the spectrofluorometer could be neglected once the spectrofluorometer has been calibrated with the standard light sources. Since these information could be derived from a power distribution profile in either an absolute scale or normalized scale. However, if the information of interest is the variation of conversion efficiency with temperature, consistency of the measurement conditions does matter. Since it requires comparison of the absolute emitted intensity (total energy) of the sample measured at identical set of conditions. A quantitative comparison of the integral emission spectral intensity of given phosphor measured at different conditions is of little scientific significance.

For a better assessment of the thermal stability of phosphors, it is advisable to measure the QE of the phosphor in question at different temperatures. If the temperature-dependent emission spectral intensity is employed as a measure for evaluating TQ performance of the phosphor, temperature-dependent excitation (absorption) and decay time of the given phosphor should also be measured to check whether the associated data are self-consistent. From an application viewpoint, if a specific phosphor possessed NTQ, it should also be verified in the prototype WLED device under practical operating temperature (drive current). Temperature dependence of the emission spectral intensity alone is not a sound metric justifying the NTQ behavior of the given phosphors.

4. Summary

In recent years, there have been huge number of literature reports on NTQ of various phosphors. Due to space limitations, this article only discusses a portion of them. However, the issues with the measurement errors originating from change in the surface state of the sample and geometrical

configuration of the spectrofluorometer due to the change of sample volume are common. It should be emphasized that these NTQ conclusions are primarily based on the temperature-dependent emission spectral intensity of the phosphor under investigation. If the enhancement of emission intensity originating from improved luminescence efficiency of given phosphors at high temperatures, the research and development of these phosphors and unraveling the mechanism underlying are undoubtedly of great significance. However, this hypothesis needs substantiation by either rigorous physical principle or practical applications. If the enhancement of the emission spectral intensity is measurement errors caused by changes in spectral measuring conditions, the experimental results are not credible and associated explanations for NTQ such as defect-related energy transfer and increased phonon numbers at high temperature, etc., were just beautiful legends.

This paper discusses the typical NTQ results reported in literature from a macroscopic viewpoint based on common sense. It is hoped to arouse the awareness in the phosphor community for the issues with the papers reporting NTQ of the specific phosphors based on spectral intensity. It is specifically emphasized that when emission spectral intensity is employed to evaluate the conversion efficiency of phosphors, keeping the same set of measurement conditions for the sample and reference standard is most important. Once the conditions have changed, comparison of the emission spectral intensity could hardly report the authentic efficiency. Special care should be paid to the consistency and stability of measuring conditions besides calibrations when a spectrofluorometer is used for quantitative analyses.

Institutional Review Board Statement: Not applicable.

Informed Consent Statement: Not applicable.

Data Availability Statement: No new data were created.

Acknowledgments: The author is grateful to KanHoo Company for financial support.

Conflicts of Interest: The author declares no conflict of interest.

References

1. Viswanath, N. S. M.; Fang, M.-H.; Huu, H. T.; Han, J. H.; Liu,R.-S. ; Im, W. B. Correlated Na^+ ion migration invokes zero thermal quenching in a sodium superionic conductor-type phosphor. *Chem. Mater*. **2022**, *34*, 107-115.
2. Kim, Y. H.; Arunkumar, P.; Kim, B. Y.; Unithrattil, S.; Kim, E.; Moon, S.-H.; Hyun, J. Y.; Kim, K. H.; Lee, D.; Lee, J.-S.; Im, W. B. A zero-thermal-quenching phosphor. *Nat. Mater*. **2017**, *16*, 543-551.
3. Li, N.; Zhang, S.; Zhao,J.; Pan,Q.; Du,Y.; Xing, B.; Li, J.; Qu W. Red shifts, intensity enhancements and abnormally thermal quenching of $Ba_9Lu_2Si_6O_{24}:Ce^{3+}$ emission by nitridation. *J. Lumin*. **2019**, *214*, 116587.
4. Shi, X.; Xue, Y.; Mao, Q.; Pei, L.; Li,X.; Liu, M.; Zhang, Q.; Zhong J. Eu^{3+} single-doped phosphor with antithermal quenching behavior and multicolor-tunable properties for luminescence thermometry. *Inorg. Chem*. **2023**, *62*, 893-903.
5. Wang, X.; Zhao, Z.; Wu,Q.; Wang, C.; Wang, Q.; Yanyan, L.; Wang,Y. Structure, photoluminescence and abnormal thermal quenching behavior of Eu^{2+}-doped $Na_3Sc_2(PO_4)_3$: a novel blue-emitting phosphor for n-UV LEDs. *J. Mater. Chem. C* **2016**, *4*, 8795-8801.
6. Liu, Z.; Zhou, T.; Yang, C.; Chen, J.; Agrawal, D. K.; Mao, Z.; Wang, D. Tunable thermal quenching properties of $Na_3Sc_2(PO_4)_3:Eu^{2+}$ phosphors tailored by phase transformation details. *Dalton Trans*. **2020**, *49*, 3615-3621.
7. Yan, J.; Zhang, Z.; Milićevića, B.; Li, J.; Liang, Q.; Zhou, J.; Wang, Y.; Shi, J.; Wu M. The enhancement of emission intensity and enlargement of color gamut by a simple local structure substitution with highly thermal stability preserved. *Opt. Mater*. **2019**, *95*,109201.
8. Xian, Y.; Li,J.; Wen, D.; Xie, F.; Xu,Y.; Xu, P.; Zhang, Q.; Chen, Z.; Yan, J. Cation sites modification enhanced luminescence and thermal quenching characteristic in the blue light-emitting $Na_3Sc_{2-x}Zn_x(PO_4)_3:0.03Eu^{2+}$ phosphors. *J. Lumin*. **2020**,*228*,117615.
9. Qiao, J.; Ning, L.; Molokeev, M. S.; Chuang,Y.-C.; Liu,Q.; Xia, Z. Eu^{2+} site preferences in the mixed cation $K_2BaCa(PO_4)_2$ and thermally stable luminescence. *J. Am. Chem. Soc.* **2018**, *140*, 9730-9736.
10. Hu,T.; Gao,Y.; Ji, X.; Xia, Z.; Zhang, Q. Thermal quenching properties of narrow-band blue-emitting $MBe_2(PO_4)_2:Eu^{2+}$ (M = Ca, Sr) phosphors towards backlight display applications. *Inorg. Chem. Front.* **2020**, *7*, 2685-2691.

11. Tang, J.; Si, J.; Li, G.; Zhou, T.; Zhang, Z.; Cai, G. Excellent enhancement of thermal stability and quantum efficiency for $Na_2BaCa(PO_4)_2:Eu^{2+}$ phosphor based on Sr doping into Ca. *J. Alloys Compd*. **2022**, *911*, 165092.
12. Zhong, Y.; Xia, M.; Chen, Z.; Gao, P.; Hintzen, H.T.; Wong, W.-Y.; Wang, J.; Zhou Z. Pyrophosphate phosphor solid solution with high quantum efficiency and thermal stability for efficient LED lighting. *iScience* **2020**,*23*,100892.
13. Wei, Y.; Gao, Z.; Liu, S.; Chen, S.; Xing, G.; Wang, W.; Dang, P.; Kheraif, A. A. A.; Li, G.; Lin, J. Highly efficient green-to-yellowish-orange emitting Eu^{2+}-doped pyrophosphate phosphors with superior thermal quenching resistance for w-LEDs. *Adv. Optical Mater*. **2020**, *8*, 1901859.
14. Leng, Z.; Zhang, D.; Bai, H.; He, H.; Qing, Q.; Zhao, J.; Tang, Z. A zero-thermal-quenching perovskite-like phosphor with an ultra-narrow-band blue-emission for wide color gamut backlight display applications. *J. Mater. Chem. C* **2021**, *9*, 13722-13732.
15. Ding, X.; Wang, Y. Commendable Eu^{2+}-doped oxide-matrix-based $LiBa_{12}(BO_3)_7F_4$ red broad emission phosphor excited by NUV light: electronic and crystal structures, luminescence properties. *ACS Appl. Mater. Interfaces* **2017**, *9*, 23983-23994.
16. Li, G.-H.; Wu, P.-F.; Ye, B.; Cai, G.-M. Enhancement of Eu^{2+} photoluminescence behavior in $NaBaB_9O_{15}$ based on the K^+ doping. *J. Lumin*. **2022**, 243,118613.
17. Zhuo, Y.; Hariyani, S.; Zhong, J.; Brgoch, J. Creating a green-emitting phosphor through selective rare-earth site preference in $NaBaB_9O_{15}:Eu^{2+}$. *Chem. Mater*. **2021**, *33*, 3304-3311.
18. Wu, X.; Shi, R.; Zhang, J.; Wen, D.; Qiu, Z.; Zhang, X.; Zhou, W.; Yu, L.; Lian, S. Highly efficient and zero-thermal-quenching blue-emitting Eu^{2+}-activated K-beta-alumina phosphors. *Chem. Eng. J*. **2022**,*429*, 132225.
19. Piao, S.; Wang, Y.; Zhou, X.; Geng, W.; Zhang, J.; Zhang, X.; Wu, D.; Cao, Y.; Li, X.; Chen B. Defect engineering in a Eu^{2+}-doped β Al_2O_3 structure blue phosphor and its controllable zero-thermal quenching luminescence. ACS Sustainable Chem. Eng. 2021, 9, 7882-7890.
20. Shao, Q.; Lin, H.; Dong, Y.; Fu, Y.; Liang, C.; He, J.; Jiang, J. Thermostability and photostability of $Sr_3SiO_5:Eu^{2+}$ phosphors for white LED applications. *J. Solid State Chem*. **2015**, *225*,72-77.
21. Fan, X.; Chen, W.; Xin, S.; Liu, Z.; Zhou, M.; Yu, X.; Zhou, D.; Xu, X.; Qiu, J. Achieving long-term zero-thermal-quenching with the assistance of carriers from deep traps. *J. Mater. Chem. C* **2018**, *6*,2978-2982.
22. Zhang, M.; Xia, Z.; Liu, Q. Thermally stable $K_xCs_{1-x}AlSi_2O_6:Eu^{2+}$ phosphors and their photoluminescence tuning. *J. Mater. Chem. C* **2017**, *5*,7489-7494.
23. Tu, Y.-Y.; Yang, Z.-H.; Wang, C.-H.; Wang, T.-W.; Lu, F.-C. Synthesis, crystal structure, and anti-thermal quenching performance of $Lu_2Sr_{(1-x)}Al_4SiO_{12}:xEu^{2+}$ phosphors. *J. Am. Ceram. Soc.* **2022**,*105*,5240-5251.
24. Xin, S; Zhu, G. Enhanced luminescence and abnormal thermal quenching behaviour investigation of BaHfSi3O9:Eu2+ blue phosphor co-doped with La^{3+}–Sc^{3+} ion pairs. *RSC Adv*. **2016**, *6*, 41755-41760.
25. Shi, R.; Zhang, X.; Qiu, Z.; Zhang, J.; Liao, S.; Zhou, W.; Xu, X.; Yu, L.; Lian, S. Composition and antithermal quenching of noninteger stoichiometric Eu^{2+}-doped Na-β-alumina with cyan emission for near-UV WLEDs. *Inorg. Chem*. **2021**, 60, 19393-19401.
26. Hariyani, S.; Brgoch, J. Advancing human-centric LED lighting using $Na_2MgPO_4F:Eu^{2+}$. *ACS Appl. Mater. Interfaces* **2021**, *13*,16669-16676.
27. Ma, H.; Tao, S.; Hua, Y.; Zheng, J.; Lou, L.; Ping, Y.; Qiao, P. A study of negative-thermal-quenching $(Ba/Ca)AlSi_5O_2N_7:Eu^{2+}$ phosphors. *Dalton Trans*. **2021**, *50*, 17792.
28. Yin, Y.; Yang, W.; Wang, Z.; Zhang, Y.; Zhu, M.; Dou, C.; Che, Y.; Sun, S.; Hu, C.; Teng, B.; Zhao, J.; Lu,J.; Sun, R.; Zhong, D. Achieving zero-thermal quenching luminescence in $ZnGa_2O_4$: $0.02Eu^{3+}$ red phosphor. *J. Alloys Compd*. **2022**, *898*, 162786.
29. Ling, S.; Liang, J.; Yan, Y.; Luo, C.; Liao, S.; Huang, Y. A new type of zero thermal quenching red emitting phosphor β-$NaYF_4:Eu^{3+}$ for NUV LED. *J. Solid State Chem*. **2022**,*311*,123099.
30. Geng, X.; Xie, Y.; Ma, Y.; Liu, Y.; Luo, J.; Wang, J.; Yu, R.; Deng, B.; Zhou W. Abnormal thermal quenching and application for w-LEDs: Double perovskite $Ca_2InSbO_6:Eu^{3+}$ red-emitting phosphor. *J. Alloys Compd*. **2020**,847, 156249.
31. Ma, X.; Yang, S.; Shao, B.; Lv, Q.; Wang, C.; Wang, C. Defect-induced zero thermal quenching of a bright red-emitting nonlinear optical material. *New J. Chem*. **2023**, *47*,1691-1701.
32. Viswanath, N.S.M.; Grandhi, G. K.; Huu,H. T.; Choi, H.; Kim,H. J.; Kim, S. M.; Kim,H. Y.; Park, C.-J.; Im, W. B. Zero-thermal-quenching and improved chemical stability of a UCr_4C_4-type phosphor via crystal site engineering. *Chem. Eng. J*. **2021**, *420*, 127664.
33. Wei, Q.; Ding, J.; Wang, Y. A novel tunable extra-broad yellow-emitting nitride phosphor with zero-thermal-quenching property. *Chem. Eng. J*. **2020**,*386*,124004.
34. Li, Z.; Tian,T.; Yuan,W.; Cui,Q.; Zhang, Y.; Gong, Z.; Mao, C.; Liu,W.; Yang,B.; Xu,W.; Chu, Y.; Liu, L.; Xu, J. Stable zero-thermal quenching cover wide temperature range achieves in cerium doped KY_3F_{10} ultraviolet luminescent single crystal. *J. Alloys Compd.* **2022**,*908*,164651.

35. Li, Q.; Chen, C.; Qiao, Y.; Yu, B.; Shen, B.; Zhang, Y. High thermal stability of green-emitting phosphor NaBaB9O15: Tb3+ via energy compensation. *J. Alloys Compd*. **2022**,*897*,163131.
36. Deng, M.; Cao, X.; Tang, Y.; Zhou, Z.; Liu, L.; Liu, X.; Zhang, P.; Chang, L.-Y.; Ruan, H.; Guo, X.; Wang, J.; and Liu, Qn. Gradient defects mediate negative thermal quenching in phosphors. *Adv. Photonics* **2023**,5, 026001.
37. Chen, Y.; Yu, B.; Gou, J.; Liu, S. F. Zero-thermal-quenching and photoluminescence tuning with the assistance of carriers from defect cluster traps. *J. Mater. Chem. C* **2018**, *6*, 10687-10692.
38. Qian, Y.; Zhu, D.; Pu, Y. A zero-thermal-quenching phosphor $Sr_3La(AlO)_3(BO_3)_4$: Dy^{3+} for near ultraviolet excitation white-LEDs. *J. Lumin*. **2022**,*243*, 118610.
39. Wang, R.-R.; Zhang, J.; Liu, Y.-J.; Li, G.-H.; Cai, G.-M. Anti-thermal quenching phosphors based on the new phosphate host $Ca_{3.6}In_{3.6}(PO_4)_6$. *Dalton Trans*. **2023**, *52*,5552-5562.
40. Geng, X.; Xie,Y.; Chen,S.; Luo,J.; Li, S.; Wang, T.; Zhao, S.; Wang, H.; Deng,B.; Yu, R.; Zhou, W. Enhanced local symmetry achieved zero-thermal-quenching luminescence characteristic in the Ca_2InSbO_6:Sm^{3+} phosphors for w-LED. *Chem. Eng. J*. **2021**,410,128396.
41. Ye, W.; Ma, C.; Li,Y.; Zhao, C.; Wang,Y.; Zuo, C.; Wen, Z.; Li, Y.; Yuan, X.; Cao Y. Anti-thermal-quenching red-emitting $GdNbO_4$:Pr^{3+} phosphor based on metal-to-metal charge transfer for optical thermometry application. *J. Mater. Chem. C* **2021**, *9*, 15201-15211.
42. Long, Z.; Wen, Y.; Qiu, J.; Wang, J.; Zhou,D.; Zhu,C.; Lai, J.; Xu,X.; Yu, X.; Wang, Q. Crystal structure insight aided design of $SrGa_2Si_2O_8$:Mn^{2+} with multi-band and thermally stable emission for high-power LED applications. *Chem. Eng. J*. **2019**,375, 122016.
43. Han, J. H.; Viswanath, N. S. M.; Park,Y. M.; Cho, H. B.; Jang, S. Woo J.; Min, W.; Im, W. B. Zero-thermal-quenching layered metal halide perovskite. *Chem. Mater*. **2022**, *34*,5690-5697.
44. Wu, L.; Sun, S.; Bai, Y.; Xia, Z.; Wu,L.; Chen,H.; Zheng,L.; Yi, H.; Sun, T.; Kong,Y.; Zhang,Y.; Xu, J. Defect-induced self-reduction and anti-thermal quenching in $NaZn(PO_3)_3$:Mn^{2+} red phosphor. *Adv. Optical Mater*. **2021**, *9*,2100870.
45. Huang, D.; Ouyang, Q.; Kong, Y.; Wang, B.; Cheng, Z.; Kheraif, A. A. A.; Lian H.; Lin J. Highly efficient yellow emission and abnormal thermal quenching in Mn^{2+}-doped Rb_4CdCl_6. *Dalton Trans*. **2023**, *52*, 5715-5723.
46. Zhou, Z.; Zhu, H.; Huang, X.; She, Y.; Zhong, Y.; Wang, J.; Liu, M.; Li, W.; Xia, M. Anti-thermal-quenching, color-tunable and ultra-narrow-band cyan green-emitting phosphor for w-LEDs with enhanced color rendering. *Chem. Eng. J*. **2022**,*433*, 134079.
47. Beers, W. W.; Cohen, W. E.; Srivastava, A. M. Temperature dependence of Mn^{4+} emission intensity and lifetime in TriGain® phosphor (K_2SiF_6:Mn^{4+}). *ECS J. Solid State Sci. Technol*. **2023**, *12*, 116002.
48. Senden, T.; Dijk-Moes, R. J. A. ; Meijerink, A. Quenching of the red Mn^{4+} luminescence in Mn^{4+}-doped fluoride LED phosphors. *Light- Sci. Appl*. **2018**,*7*,8.
49. Shao, Q.; Wang, L.; Song, L.; Dong, Y.; Liang, C.; He, J.; Jiang, J. Temperature dependence of photoluminescence spectra and dynamics of the red-emitting K_2SiF_6:Mn^{4+} phosphor. *J. Alloys Compd*. **2017**,*695*,221-226.
50. Tang, F.; Su, Z.; Ye,H.; Gao, W.; Pan,X.; Xu, S. Large negative-thermal-quenching effect in phonon-induced light emissions in Mn^{4+}-activated fluoride phosphor for warm-white light-emitting diodes. *ACS Omega* **2018**, *3*,13704-13710.
51. Zhu, H.; Lin,C. C.; Luo,W.; Shu, S.; Liu, Z.; Liu,Y.; Kong,J.; Ma,E.; Cao,Y.; Liu, R.-S. ; Chen, X. Highly efficient non-rare-earth red emitting phosphor for warm white light-emitting diodes. *Nat. Commun*. **2014**, *5*,4312.
52. Zhou, Q.; Zhou, Y.; Wang, Z.; Liu, Y.; Chen, G.; Peng, J.; Yan, J.; Wu, M. Fabrication and application of non-rare earth red phosphors for warm white-light-emitting diodes. *RSC Adv*. **2015**, *5*, 84821-84826.
53. Adachi, S. Investigation on anomalous thermal quenching of Mn^{4+} luminescence in A_2XF_6:Mn^{4+}. *ECS J. Solid State Sci. Technol*. **2021**, *10*, 076007.
54. Adachi, S. Negative thermal quenching of Mn^{4+} luminescence in fluoride phosphors: effects of the $^4A_{2g} \rightarrow {}^4T_{2g}$ excitation transitions and normal thermal quenching. *ECS J. Solid State Sci. Technol*. **2022**,*11*,036001.
55. Zhang, D.; Zhou, J.; Cao,X.; Ge,X.; Tang, F.; Zheng,C.; Ning, J.; Xu, S. Manipulation of temperature-dependent luminescence behaviors of Mn^{4+}-activated fluoride phosphors. *J. Phys. Chem. Lett.* **2023**, *14*, 6464-6469.
56. Deng, T.; Zhang, S.; Zhou, R.; Yu,T.; Wu, M.; Zhang, X.; Chen, K.; Zhou, Y. Defect-related luminescence behavior of a Mn^{4+} non-equivalently doped fluoroantimonate red Phosphor. *Dalton Trans*. **2022**, 51, 608-617.
57. Yang, X.; Liao, C.; Jin, Z.; Wang, Q.; Xie, W.; Yang, P.; Wang, Z. Luminescent properties of Mn^{4+} in an oxyfluoride complex with ultra-high thermal stability. *Mater. Res. Bull*. **2022**,*150*,111798.

58. Wang, C.; Cai, Y.; Zhang, H.; Liu, Z.; Lv, H.; Zhu,X.; Liu,Y.; Wang,C.; Qiu, J.; Yu,X.; Xu, X. Variation from zero to negative thermal quenching of phosphor with assistance of defect states. *Inorg. Chem.* **2021**, *60*, 19365-19372.
59. Wei, Y.; Yang, H.; Gao, Z.; Yun, X.; Xing, G.; Zhou, C.; Li, G. Anti-thermal-quenching Bi^{3+} luminescence in a cyan-emitting $Ba_2ZnGe_2O_7$:Bi phosphor based on zinc vacancy. *Laser Photonics Rev*. **2021**,*5*, 2000048.
60. Li, H.; Cai, J.; Pang, R.; Zhang, S.; Jiang, L.; Li, D.; Li, C.; Feng, J.; Zhang, H. A strategy for developing thermal-quenching resistant emission and super-long persistent luminescence in $BaGa_2O_4:Bi^{3+}$. *J. Mater. Chem. C* **2019**,*7*,13088-13096.
61. Ma, Q.; Guo, N.; Xin, Y.; Shao, B. Preparation of zero-thermal-quenching tunable emission bismuth-containing phosphors through the topochemical design of ligand configuration. *Inorg. Chem. Front*. **2021**, *8*,4072-4085.
62. Yang, S.; Wu, Y.; Yue, F.; Qi, R.; Jiang, B.; Wu,J.; Shen, Y.; Duan, C.; Shan, Y.; Zhao, Q.; Zhang, Y. $MGa_2B_2O_7:Bi^{3+},Al^{3+}$ (M = Sr, Ba) blue phosphors with a quantum yield of 99% and negative thermal quenching. *Inorg. Chem. Front*. **2021**, *8*,4257-4266.
63. Wang, Z.; Lin, H.; Zhang, D.; Hong, R.; Tian,Y.; Chen, J.; Zhou, S. Reidinger defects induced thermally stable green emission from Eu2+, Mn2+ co-doped Ba0.75Al11O17.25 transparent ceramics. *J. Eur. Ceram. Soc*. **2022**,*42*,266-273.
64. Zhong, J.; Zhou, Y.; Hariyani, S.; Zhao,W.; Zhuang,W.; Brgoch, J. Thermally robust and color-tunable blue-green-emitting $BaMgSi_4O_{10}:Eu^{2+},Mn^{2+}$ phosphor for warm-white LEDs. *Inorg. Chem*. **2020**, *59*, 13427-13434.
65. Shi, R.; Cao, S.; Han, Y.; Zhang, J.; Zhang,X.; Liao, S.; Lian, S. Defect and energy transfer induced abnormal thermally stable and highly efficient narrow-band green emission. *Appl. Mater. Today* **2022**, *29*,101625.
66. Zhu, H.; Huang, X.; Li, Y.-N.; She, Y.-l.; Wang, J.; Wong,W.-Y.; Liu, M.; Li,W.; Zhou, Z.; Xia, M. Novel ultra-high-temperature zero-thermal quenching plant-protecting type blue-green dual-emission $KAl_{11}O_{17}:Eu^{2+},Mn^{2+}$ phosphors for urban ecological lighting. *J. Mater. Chem. C* **2022**, *10*, 3461-3471.
67. Liu, D.; Wang, T.; Liu, Y.; Wang,C.; Liu,Z.; Zhu, X.; Liu, Y.; Zhang, J.; Teng, Z.; Zhong, Y.; Nikolaevich, Y. A.; Xu, X. Zero-thermal-quenching of $LiAl_5O_8$: Eu^{2+}, Mn^{2+} phosphors by energy transfer and defects engineering. *Ceram. Inter*. **2023**,49,10273-10279.
68. Liu, Y.; Zhang, G.; Huang, J.; Tao, X.; Li, G.; Cai, G. Daylight-white-emitting and abnormal thermal antiquenching phosphors based on a layered host $SrIn_2(P_2O_7)_2$. *Inorg. Chem*. **2021**, *60*, 2279-2293.
69. Ling, S.; Qin, X.; Yan, Y.; Chen,C.; Meng, K.; Ming, J.; Liao, S.; Huang, Y.; Hou, L. Crystal defect induced zero thermal quenching β-$NaYF_4$: Eu^{3+}, Sm^{3+} red-emitting phosphor. *RSC Adv*. **2023**, *13*, 534-546.
70. Jiao, M.; Dong, L.; Xu, Q.; Zhang, L.; Wang, D.; Yang, C. The structures and luminescence properties of $Sr_4Gd_3Na_3(PO_4)_6F_2:Ce^{3+},Tb^{3+}$ green phosphors with zero-thermal quenching of Tb^{3+} for WLEDs. *Dalton Trans*. **2020**, 49,667-674.
71. Liu, D.; Jin, Y.; Lv, Y.; Ju,G.; Wang,C.; Chen, L.; Luo,W.; Hu, Y. A single-phase full-color emitting phosphor $Na_3Sc_2(PO_4)_3:Eu^{2+}/Tb^{3+}/Mn^{2+}$ with near-zero thermal quenching and high quantum yield for near-UV converted warm w-LEDs. *J. Am. Ceram. Soc*.**2018**,*101*,5627-5639.
72. Shi, R.; Ning, L.; Wang, Z.; Chen, J.; Sham,T.-K.; Huang, Y.; Qi, Z.; Li, C.; Tang,Q.; Liang, H. Zero-thermal quenching of Mn2+ red luminescence via efficient energy transfer from Eu^{2+} in $BaMgP_2O_7$. *Adv. Optical Mater*. **2019**,*7*, 1901187.
73. Zhang, B.-B.; Chen,J.-K.; Ma, J.-P.; Jia, X.-F.; Zhao, Q.; Guo,S.-Q.; Chen, Y.-M.; Liu,Q.; Kuroiwa,Y.; Moriyoshi, C.; Zhang, J.; Sun, H.-T. Antithermal quenching of luminescence in zero-dimensional hybrid metal halide solids. *J. Phys. Chem. Lett*. **2020**, *11*, 2902-2909.
74. Kahmann,S.; Nazarenko, O.; Shao, S.; Hordiichuk, O.; Kepenekian, M.; Even, J.; Kovalenko, M.V.; Blake, G. R.; Loi, M. A. Negative thermal quenching in $FASnI_3$ perovskite single crystals and thin films. *ACS Energy Lett*. **2020**, *5*, 2512-2519.
75. Wei, Y.; Yang,H.; Gao, Z.; Liu,Y.; Xing, G.; Dang, P.; Abdulaziz Kheraif,A. A.; Li, G.; Lin, J.; Liu, R.-S. Strategies for designing antithermal-quenching red phosphors. *Adv. Sci.* **2020**, *7*, 1903060.
76. Yang, C.; Guo, N.; Qu, S.; Ma, Q.; Liu,J.; Chen, S.; Ouyang, R. Design of anti-thermal quenching Pr^{3+}-doped niobate phosphors based on a charge transfer and intervalence charge transfer band excitation-driven strategy. *Inorg. Chem. Front*. **2023**,*10*, 4808-4818.
77. Xiao, Y.; Hao, Z. Comment on "Zero-thermal-quenching and photoluminescence tuning with assistance of carriers from defect cluster traps'' by Chen et al., J. Mater. Chem. C, 2018, 6, 10687-10692. *J. Mater. Chem. C* **2020**,*8*, 1151-1152.
78. Yan, S. Comment on "Tunable thermal quenching properties of $Na_3Sc_2(PO_4)_3:Eu^{2+}$ phosphors tailored by phase transformation details" by Liu et al., Dalton Trans. 2020,49,3915. *Dalton Trans*. **2020**,*49*,11772-11774.
79. Yan, S. Comment on "Investigation on anomalous thermal quenching of Mn^{4+} luminescence in $A_2XF_6:Mn^{4+}$" [ECS J. Solid State Sci. Technol. 10, 076007 (2021)]. *ECS J. Solid State Sci. Technol*. **2021**, *10*,120001.

80. Yan, S. On the anomalous thermal quenching of Mn^{4+} luminescence in $A_2XF_6:Mn^{4+}$ (A =K, Na, Rb or Cs; X = Si, Ti, Ge, Sn, Zr or Hf). *ECS J. Solid State Sci. Technol.* **2020**, *9*,106004.
81. Yan, S. On the validity of the defect-induced negative thermal quenching of Eu^{2+}-doped phosphors. *ECS J. Solid State Sci. Technol*. **2023**, *12*, 016001.
82. Wang, L.; Wand, X.; Kohsei, T.; Yoshimura,K.-i.; Izumi, M.; Hirosaki, N.; Xie, R.-J. Highly efficient narrow-band green and red phosphors enabling wider color-gamut LED backlight for more brilliant displays. *Opt. Express* **2015**, *23*,28707-28717.
83. Senden, T.; Geitenbeek, R. G.; Meijerink, A. Co-precipitation synthesis and optical properties of Mn^{4+}-doped hexafluoroaluminate w-LED phosphors. *Materials* **2017**, *10*, 1322.
84. Wei, L.-L.; Lin, C. C.; Wang, Y.-Y.; Fang, M.-H.; Jiao, H.; Liu, R.-S. Photoluminescent evolution induced by structural transformation through thermal treating in the red narrow-band phosphor $K_2GeF_6:Mn^{4+}$, *ACS Appl. Mater. Interfaces* **2015**, *7*, 20, 10656-10659.
85. Setlur, A. A.; Radkov, E. V. ; Henderson, C. S.; Her, J.-H.; Srivastava, A. M.; Karkada, N.; Kishore, M. S.; Kumar, N. P.; Aesram, D.; Deshpande, A.; Kolodin,B.; Grigorov, L. S.; Happek, U. Energy-efficient, high-color-rendering LED lamps using oxyfluoride and fluoride phosphors. *Chem. Mater*. **2010**, *22*, 13, 4076-4082.
86. Sun, X.-Y.; He, Z.; Gu, X. Synthesis, deep red emission and warm WLED applications of $K_2SiF_6:Mn^{4+}$ phosphors. *J. Photochem. Photobiol. A: Chem*. **2018**,*350*, 69-74.
87. Hou, Z.; Tang, X.; Luo, X.; Zhou, T.; Zhang, L.; Xie, R.-J. A green synthetic route to the highly efficient K2SiF6:Mn4+ narrow-band red phosphor for warm white light-emitting diodes. *J. Mater. Chem. C* **2018**,*6*, 2741-2746.
88. Sijbom, H. F.; Joos, J. J.; Martin, L. I. D. J.; Eeckhout, K. V.; Poelman, D.; Smet, P. F. Luminescent behavior of the K2SiF6:Mn4+ red phosphor at high fluxes and at the microscopic level. *ECS J. Solid State Sci. Technol.* **2016**,*5* (1), R3040-R3048.
89. Beers, W.W.; Smith, D. ; Cohen, W.E.; Srivastava A.M. Temperature dependence (13–600 K) of Mn^{4+} lifetime in commercial $Mg_{28}Ge_{7.55}O_{32}F_{15.04}$ and K_2SiF_6 phosphors. *Opt. Mater*. 2018,84,614-617.
90. Solé, J. G.; Bausá, L.E.; Jaque D. An introduction to the optical spectroscopy of inorganic solids. 2005 John Wiley & Sons, Ltd, pp.161-170.
91. Paschotta, R. Encyclopedia of laser physics and technology, Vol. 1 & 2. Wiley Online Library, 2008, 856.
92. Blasse, G.; Grabmeier, B. C. Luminescent materials, 1st ed., Springer, Berlin,1994.
93. Ronda, C. Luminescence, Wiley-VCH Verlag GmbH & Co. KGaA, Weinheim ,2008.
94. Smet, P. F.; Parmentier, A. B.; Poelman, D. Selecting conversion phosphors for white light-emitting diodes. *J. Electrochem. Soc*. **2011**, *158* (6), R37-R54.
95. Yan, S. On the origin of temperature dependence of the emission maxima of Eu^{2+} and Ce^{3+}- activated phosphors. *Opt. Mater*. **2018**,*79*, 172-185.
96. Bispo-Jr,A. G.; Saraiva, L. F.; Lima, S. A.M.; Pires, A. M.; Davolos, M. R. Recent prospects on phosphor-converted LEDs for lighting, displays, phototherapy, and indoor farming. *J. Lumin*. **2021**,*237*,118167.
97. Li, Y.; Deng, D.; Wang, T.; Yu, Y.; Zhong, X.; Wu, D.; Liao, S.; Huang, Y. Negative thermal quenching of $K_3AlF_6:Mn^{4+}$@GQDs phosphors caused by enhancement of the conversion of heat energy into light energy. *J. Mater. Sci: Mater Electron* **2021**, *32*,26384-26396.
98. Song, E.; Wang, J.; Shi, J.; Deng, T.; Ye, S.; Peng, M.; Wang, J.; Wondraczek, L.; Zhang, Q.; Highly efficient and thermally stable $K_3AlF_6:Mn^{4+}$ as a red phosphor for ultra-high performance warm-white LEDs, *ACS Appl. Mater. Interfaces* **2017**, *9*, 8805-8812.
99. Dat, L.Q.; Lan, N. T.; Lien, N.T.K.; Quang, N.V.; Anh, C.V. ; Tinh, N.H.; Duyen, N.T.; Thoa,V.T.K.; Hanh, N.T.; Huong, P.T.L.; Tu, N.; Nguyen, D.H. Excellent hydrophobic property of $K_3AlF_6:Mn^{4+}$ phosphor by coating with reduction graphene oxide on the surface of materials. *Opt. Mater*. **2022**, *129*, 112552.
100. (a) Mccamy, C. S. Correlated color temperature as an explicit function of chromaticity coordinates. *Color Res. Appl*. **1992**,*17*,142-144; (b) Mccamy, C. S. Correlated color temperature as an explicit function of chromaticity coordinates (Erratum). *Color Res. Appl*. **1993**,*18*,150.
101. Shchekin, O. B.; Schmidt, J.; Jin, F.; Lawrence, N.; Vampola, K. J.; Bechtel, H.; Chamberlin, D. R.; Mueller-Mach,R.; Mueller, G. O. Excitation dependent quenching of luminescence in LED phosphors. *Phys. Status Solidi RRL* **2016**, *10*,310-314.
102. Jansen, T.; Bohnisch, D.; Justel, T. On the photoluminescence linearity of Eu2+ based LED phosphors upon high excitation density. *ECS J. Solid State Sci. Technol*. **2016**, *5*, R91-R97.
103. Yan, S. On the origin of diminishing radiative lifetime of Mn4+ in complex fluoride phosphors with temperature. *ECS J. Solid State Sci. Technol.* **2021**, *10*, 086005.
104. Haar, M. A.; Tachikirt, M.; Berends, A. C.; Krames, M. R.; Meijerink, A.; Rabouw, F. T. Saturation mechanisms in common LED phosphors. *ACS Photonics* **2021**, *8*,1784-1793.
105. Bicanic, K. T.; Li, X.; Sabatini, R. P.; Hossain, N.; Wang, C.-F.; Fan, F.; Liang, H.; Hoogland, S.; Sargent, E. H. Design of phosphor white light systems for high-power applications. *ACS Photonics* **2016**, *3*,2243-2248.

106. Piquette, A.; Bergbauer, W.; Galler, B.; Mishra, K. C. On choosing phosphors for near-UV and blue LEDs for white light. *ECS J. Solid State Sci. Technol*. **2016**, *5*, R3146-R3159.
107. Du, F.; Zhuang, W.; Liu, R. ; Liu, Y.; Gao,W.; Zhang, X.; Xue, Y.; Hao, H. Synthesis, structure and luminescent properties of yellow phosphor $La_3Si_6N_{11}:Ce^{3+}$ for high power white-LEDs. *J. Rare Earths* **2017**,*35*,1059-1064.
108. Liu, L.; Fu, L.; Wu, D.; Peng, J.; Wang, R.; Du, F.; Ye, X. Effect of various cerium sources on the emission intensity of Ce3+-doped $La_3Si_6N_{11}$ phosphor for high-power white light emitting diodes. *Physica B* **2021**,*603*,412779.
109. Ueda, J.; Tanabe, S.; Takahashi, K.; Takeda, T.; Hirosaki, N. Thermal quenching mechanism of CaAlSiN3:Eu2+ red phosphor. *Bull. Chem. Soc. Jpn*.**2018**, *91*,173-177.
110. Tsai, Y.-T.; Chiang, C.-Y.; Zhou, W.; Lee, J.-F.; Sheu, H.-S.; Liu, R.-S. Structural ordering and charge variation induced by cation substitution in (Sr,Ca)$AlSiN_3$:Eu phosphor. *J. Am. Chem. Soc*. **2015**, *137*,8936-8939.
111. Arjoca, S.; Villora, E. G.; Inomata, D.; Aoki, K.; Sugahara Y.; Shimamura, K. Temperature dependence of Ce:YAG single-crystal phosphors for high-brightness white LEDs/LDs. *Mater. Res. Express* **2015**,*2*, 055503.
112. Robbin, D. J. The effects of crystal field and temperature on the photoluminescence excitation efficiency of Ce^{3+} in YAG. *J. Electrochem. Soc*. **1979**,*126*,1550-1555.
113. Wittlin, A.; Przybylińska, H.; Berkowski, M.; Kamińska, A.; Nowakowski, P.; Sybilski, P.; Ma, C.-G.; Brik, M.G.; Suchocki, A. Ambient and high pressure spectroscopy of Ce^{3+} doped yttrium gallium garnet. *Opt. Mater. Exp*. **2015**, *5*(8),1868-1880.
114. Seto, T.; Kijima, N.; Hirosaki, N. A new yellow phosphor $La_3Si_6N_{11}:Ce^{3+}$ for white LEDs. *ECS Trans*. **2009**,*25* (9), 247-252.
115. Chen, L.; Fei, M.; Zhang, Z.; Jiang, Y.; Chen, S.; Dong, Y.; Sun, Z.; Zhao, Z.; Fu, Y.; He, J.; Li, C.; Jiang, Z. Understanding the local and electronic structures toward enhanced thermal stable luminescence of $CaAlSiN_3:Eu^{2+}$. *Chem. Mater*. **2016**, *28*,5505-5515.
116. Song, Z.; Zu, R.; Liu, X.; He, L.; Liu, Q. Analysis on stability and consistency of intensity measurement of white light emitting diode phosphors. *Optik* **2016**, *127*, 2798-2801.
117. Würth, C.; Grabolle, M.; Pauli, J.; Spieles M.; Resch-Genger, U. Relative and absolute determination of fluorescence quantum yields of transparent samples, *Nature Protocols* **2013**,*8*(8),1535-1550.
118. Huang, K.; Deng, T.; Yan, S.; Hu, J. Effect of strontium and phosphorus source on the structure, morphology and luminescence of $Sr_5(PO_4)_2SiO_4:Eu^{2+}$ phosphor prepared by solid-state reaction. *Ceram. Inter*. **2013**,*39*,6713-6720.
119. Tsai, Y.-T.; Huang, Y. S.; Majewsk, N.; Mahlik, S.; Muchlis, A. M. G.; Huang, Y.-K.; Huang, Y. L.; Lin,B.-H.; Su,C.; Lin, C. C. Shielding effect and compensation defect study on $Na_3Sc_2(PO_4)_y:Eu^{2+,3+}$ (y = 2.6–3.0) phosphor by anion-group-induced phase transition. *J. Mater. Chem. C* **2022**,*10*,15044-15050.
120. Rohwer, L. S.; Martin, J. E. Measuring the absolute quantum efficiency of luminescent materials. *J. Lumin*. **2005,** *115*, 77- 90.
121. Leyre, F. S.; Coutino-Gonzalez, E.; Joos, J. J.; Ryckaert, J. ; Meuret, Y.; Poelman, D.; Smet, P. F. ; Durinck, G.; Hofkens, J.; Deconinck G.; Hanselae, P. Absolute determination of photoluminescence quantum efficiency using an integrating sphere setup, *Rev. Sci. Instrum*. **2014**,*85*, 123115.
122. Würth, C.; Grabolle, M.; Pauli, J.; Spieles, M.; Resch-Genger, U. Comparison of methods and achievable uncertainties for the relative and absolute measurement of photoluminescence quantum yields. *Anal. Chem.* **2011**, *83*, 3431-3439.